



ORIGINAL ARTICLE

Diagnostic product ions-based chemical characterization and antioxidative activity evaluation of solid fermentation for Astragali radix produced by *Paecilomyces cicadae*



Zihan Liu^{a,b}, Shaoping Wang^a, Qiyang Li^c, Fan Dong^a, Haoran Li^a, Zhibin Wang^d, Long Dai^a, Xia Wei^{c,*}, Jiayu Zhang^{a,*}

^a School of Pharmacy, BIN ZHOU Medical University, 264003, China

^b School of Chinese Pharmacy, Beijing University of Chinese Medicine, Beijing 102488, China

^c Shandong Institute for Food and Drug Control, Jinan 250101, China

^d Tongrentang Research Institute, Beijing 100079, China

Received 8 September 2020; accepted 4 November 2020

Available online 16 November 2020

KEYWORDS

Solid fermentation for Astragali radix produced by *Paecilomyces cicadae* (SF-AP);
Chemical transformation;
Diagnostic product ions (DPIs);
Antioxidative activity;
Ultra-high performance liquid chromatography-linear ion trap-Orbitrap mass spectrometry (UHPLC-LTQ-Orbitrap MS)

Abstract Studies on herbal medicines and fermentation products have become increasingly essential with the development of modern industry and technology. In order to verify that fermentation can bring about changes, *Paecilomyces cicadae* [*Paecilomyces cicadae* (Miquel.) Samson] was used to ferment Astragali radix [Astragalus membranaceus (Fisch.) Bge. var. mongho-licus (Bge.) Hsiao]. After solid fermentation for Astragali radix produced by *Paecilomyces cicadae* (SF-AP) was established, an efficient strategy based on ultra-high performance liquid chromatography-linear ion trap-Orbitrap mass spectrometry (UHPLC-LTQ-Orbitrap MS) was developed to screen and identify the chemical transformations in SF-AP and Astragali radix according to the acquired diagnostic product ions (DPIs). As a result, 114 compounds including 45 saponins and 69 flavonoids were finally identified and validated. Moreover, two kinds of antioxidative tests corresponding to the scavenging of DPPH[•] and ABTS^{•+} were applied to evaluate the antioxidative activity of Astragali radix before and after fermentation. The results demonstrated that some significant chemical transformations such as relative content fluctuations and structural isomerism owing to the

* Corresponding authors.

E-mail addresses: myweixia@126.com (X. Wei), zhangjiayu0615@163.com (J. Zhang).

Peer review under responsibility of King Saud University.



occurrence of hydrolysis and conversion reactions and the antioxidative activity of SF-AP was much higher than that of the Astragali radix. This study could provide a new method for the utilization of Astragali radix and constructive guidance for the further research of fermented herbal medicines.

© 2020 The Authors. Published by Elsevier B.V. on behalf of King Saud University. This is an open access article under the CC BY license (<http://creativecommons.org/licenses/by/4.0/>).

1. Introduction

Microbial fermentation has already been applied in the processing of herbal medicines and functional food for thousands of years, such as Banxiaqu (pinellia ternata fermented mass) and Dandouchi (sojae semen praeparatum). Previous studies have demonstrated that fermentation plays an important role in toxicity reducing and efficacy enhancing (Ming et al., 2017). The prime reason was that microorganisms could generate sorts of important secondary metabolic products, and the macromolecular constituents could be decomposed into small molecules during the process (Hussain et al., 2016; Stanton et al., 2005; Xu et al., 2015).

As annual or perennial herb or shrub that is prevalently distributed in temperate and arid areas, Astragali radix [Astragalus membranaceus (Fisch.) Bge. var. mongholicus (Bge.) Hsiao] belonging to the popular genera of plants in Leguminosae, has been widely used in herbal medicines for over 2,000 years. It contains saponins, flavonoids, etc, which are known for their anti-inflammatory, anti-oxidant, and other pharmacological effects (Fu et al., 2015). It is commonly used as food and beverage additive and nutritional dietary supplement to enhance the body's resistance against various diseases in numerous Asian countries. In terms of *Paecilomyces cicadae* [Paecilomyces cicadae (Miquel.) Samson], one kind of fungus owing high nutritional and medical value is formed by paecilomyces parasitizing the nymphs of cicadas. Modern pharmacological studies have showed that it had similar clinical effects to Cordyceps just like regulating immunity, improving the kidney function, strengthening with tonics, anti-oxidation, anti-tumor and anti-virus, etc (Zhao et al., 2018a, 2018b; Zhang et al., 2017).

In the preliminary report, and as part of our long-term investigation for fermentation, we have described the chemical constituent profiling and lowering uric acid activity of *Paecilomyces cicadae* liquid fermentation for Astragali Radix (Wang et al., 2019a, Wang et al., 2019b). Compared with the previous study of *Paecilomyces cicadae* liquid fermentation for Astragali Radix, we found that the distinguishment between solid fermentation and liquid fermentation lies in the difference of medium state. The concept of solid fermentation covers a wide range, including the fermentation mode of suspending insoluble solid substances in liquid (also known as carrier culture) and cultivating microorganisms on wet solid materials with almost no flowable water. There are a great many advantages of solid fermentation, such as simple operation, low energy consumption, easy domination, less pollution, and so on. Nowadays, modern fermentation technology has been gradually changed from traditional natural fermentation that relying on production experience to pure strain fermentation, which represents fermentation technology and system are

becoming increasingly mature (Martins et al., 2011; Singhania et al., 2009; Wang et al., 2016; Liu et al., 2004).

In order to prove that the fermentation process can some cause favorable chemical changes, an ultra-high performance liquid chromatography-linear ion trap-Orbitrap mass spectrometry (UHPLC-LTQ-Orbitrap MS) method coupled with the assistance of diagnostic product ions (DPIs) analysis was developed to characterize the chemical transformation and further obtain a comprehensive knowledge about constituents in the established SF-AP system. Meanwhile, two antioxidative tests including DPPH[·] scavenging activity and ABTS^{·+} scavenging activity were utilized to evaluate the antioxidative effects of Astragali radix before and after solid fermentation.

2. Experimental

2.1. Chemicals and materials

The identity of Astragali radix was authenticated by histological and morphological methods according to monograph of Chinese Pharmacopoeia (version 2015) by Prof. Long Dai in BIN ZHOU Medical University (Yantai city, Shandong). *Paecilomyces cicadae* (Miquel) Samson (No. cfcc81169) was provided by China Forestry Culture Collection Center (Beijing, China). A total of thirteen reference substances including six triterpene saponins, i.e. β -D-Glucopyranoside, (3 β , 6 α , 16 β , 20R, 24S)-3-[(3, 4-di-O-acetyl- β -D-xylopyranosyl)oxy]-20, 24-epoxy-16, 25-dihydroxy-9, 19-cyclolanostan-6-yl, Astragaloside I, Astragaloside II, Astragaloside IV, Isoastragaloside I, Isoastragaloside II and seven flavonoids, i.e. Calycosin, Genistin, Complanaraside, Formononetin, Ononin, Astraisoflavan-7-O- β -D-glucoside and Isoquercitrin, were all purchased from Chengdu Must Biotechnology Co. Ltd. (Sichuan, China). The structures were fully elucidated by comparing the ESI-MS, ¹H NMR and ¹³C NMR spectra data with the published literature. All of their purities were acceptable ($\geq 98\%$) according to HPLC-UV analysis.

Acetonitrile, methanol and formic acid of LC-MS grade were all purchased from Thermo Fisher Scientific (Fair Lawn, NJ, USA). 2, 2'-azino-bis (3-ethylbenzothiazoline-6-sulfonic acid) (ABTS), 1, 1-diphenyl-2-picrylhydrazyl (DPPH), Potassium persulfate (K₂S₂O₈) were obtained from Shanghai Macklin Biochemical Co., Ltd (Shanghai, China). All the other chemicals of analytical grade were provided by Beijing Chemical Works (Beijing, China). Deionized water used throughout the experiment was purified by Milli-Q Gradient A 10 System (Millipore, Billerica, MA, USA). Grace PureTM SPE C18-Low solid-phase extraction cartridges (200 mg/3 mL, 59 μ m, 70 Å) were purchased from Grace Davison Discovery Science (Deerfield, IL, USA).

2.2. The preparation of SF-AP system

2.2.1. Fungus activation and liquid culture

Paecilomyces cicadae was inoculated on potato liquid medium in 500 mL conical flask, and then it was cultured in an incubator with constant temperature and humidity to activate it by setting parameters at 27°C and relative humidity of 80% for 5 days. Activated *Paecilomyces cicadae* were selected by inoculation ring and cultured in potato liquid medium at 25°C and 140 r/min for 7 days.

2.2.2. Solid-state fermentation

The powder (5 g) of Astragali radix was placed in 250 mL conical bottle and then soaked with 6 mL distilled water. After that, the conical bottle loaded with wet medicinal powder was sterilized at 121 °C for 30 min. 3 mL liquid spawn of activated *Paecilomyces cicadae* was inoculated and cultured in a solid fermentation flask with constant temperature of 26 °C and humidity of 90%. Astragali radix were ground into powder passing with 100 mesh sieve and cultured for 14 days at 26 °C under aerobic conditions.

2.3. Analytical sample preparation

SF-AP samples were taken on the 14th day for the subsequent analyses. Then they were ground into powder passing 100 mesh sieve. Furthermore, the above two powder samples were respectively dissolved in methanol at a concentration of 100 mg/mL. Samples were ultrasonic extracted for 35 min and then the solutions were evaporated. After concentration, the initial mobile phase was used to resolve these two samples.

SF-AP (1 mL) and Astragali radix (1 mL) solution was respectively added into the SPE cartridges, which were orderly pretreated with 5 mL methanol and 5 mL deionized water. Afterwards, the SPE cartridges were successively washed with 3 mL deionized water and 3 mL methanol. The methanol eluate was evaporated to dryness by water bath. Then the residue was redissolved in 200 µL methanol solution and centrifuged for 30 min (13,500 rpm, 4 °C). The supernatant was finally used for the subsequent analysis.

2.4. Instrument and conditions

UHPLC analysis was performed on DIONEX Ultimate 3000 UHPLC system (Thermo Fisher Scientific, MA, USA), which was equipped with a binary pump, an auto-sampler and a column compartment. The chromatographic separation was carried out at 40 °C using Waters ACQUITY HSS T3 column (2.1 × 100 mm i.d., 1.8 µm; Waters Corporation, Milford, MA, USA). The mobile phase consisted of 0.1% formic acid aqueous solution (A) and acetonitrile (B) at a flow rate of 0.2 mL/min. The linear gradient procedure was described as follows: 0–6 min, 8%–25% B; 6–13 min, 25%–32% B; 13–20.5 min, 32%–48% B; 20.5–26 min, 38%–44% B; 26–30 min, 44%–92% B. The injection volume was 3 µL.

HRMS spectral analysis was executed on LTQ-Orbitrap XL mass spectrometer (Thermo Fisher Scientific, MA, USA). The optimized operating parameters in negative and positive ion modes were set as follows: sheath gas flow rate of 40 arb, auxiliary gas flow rate of 20 arb, capillary voltage

of ± 25 V, electrospray voltage of 3.0 kV, tube lens of ± 110 V, and capillary temperature of 350 °C. The components were detected using full-scan MS analysis from *m/z* 100–1,200 with a resolution of 30,000 in both positive and negative ion modes. The collision energy for collision induced dissociation (CID) was set to 40%.

2.5. Peak selections and data processing

Thermo Xcalibur 2.1 workstation (Thermo Fisher Scientific, MA, USA) was used for data acquisition and processing. In order to acquire as many fragment ions as possible, this method targeted the peaks with intensity over 10,000 for the subsequent structural identification. The predicted atoms for chemical formulas of all the deprotonated molecular ions were set as follows: C [0–50], H [0–100], O [0–30], N [0–1] and Ring Double Bond (RDB) equivalent value [0–15]. The maximum mass errors between the measured and calculated values were fixed within ± 5 ppm.

2.6. Determination of antioxidative capacity in vitro

2.6.1. Sample preparation

The two powder samples (Astragali radix and SF-AP), each weighting 3 g, were respectively suspended in 50 mL of 80% methanol solution. Each sample was sonicated for 45 min and centrifuged at 5,000 rpm for 10 min. Then the supernatant fraction was filtrated to obtain extraction solution. Subsequently, the two kinds of extraction solutions were diluted to different concentrations for the determination of antioxidative activity *in vitro*.

2.6.2. DPPH[·] scavenging activity assay

DPPH[·] solution (0.5 mmol/L) was prepared and then 1 mL was respectively added into various Astragali radix and SF-AP concentrations (1 mL). The mixed solutions were incubated at 25 °C for 30 min and protected from light. Finally, the absorbances of these sample solutions were measured at 517 nm (Zeng et al., 2012). DPPH[·] scavenging activity was calculated as shown in formula (1).

$$\text{Scavenging of DPPH}^{\cdot} = (1 - A1/A0) \times 100\% \quad (1)$$

(A0 was the absorbance of DPPH and methanol solution; A1 was the absorbance of DPPH and sample solution)

2.6.3. ABTS^{·+} scavenging activity assay

An ABTS^{·+} stock solution was prepared by mixing 7 mmol/L ABTS with 2.45 mmol/L K₂S₂O₈ in water, which was placed in the dark at room temperature for 16 h to obtain a dark blue solution (Hsu et al., 2011). The ABTS^{·+} stock solution should be diluted with absolute ethanol before the experiment.

Two kinds of sample solutions were diluted in different concentrations, and then 1 mL of these samples were respectively taken into the ABTS^{·+} solution (2 mL). After the reaction lasted for 6 min at room temperature, the absorbances of these sample solutions were determined at 734 nm. ABTS^{·+} scavenging activity was calculated as shown in formula (2).

$$\text{Scavenging of ABTS}^{\cdot+} = (1 - A1/A0) \times 100\% \quad (2)$$

(A0 was the absorbance of ABTS and methanol solution; A1 was the absorbance of ABTS and sample solution.)

3. Results and discussion

3.1. The establishment of analytical strategy

In the present study, the analytical strategy we established included five steps. The first step was to establish the solid-state fermentation system by activating fungus and culturing liquid. Secondly, the samples of SF-AP and Astragali radix were respectively prepared into two solutions and then pre-treated by SPE cartridge for the subsequent analytical experiments. Thirdly, a sensitive and validated method based on UHPLC-LTQ-Orbitrap mass spectrometer was developed for the comprehensive analysis of chemical constituents in SF-AP and Astragali radix. The structures of the representative constituents were elucidated according to the accurate mass measurement, fragmentation patterns, DPIs and literature reports. Fourthly, the chemical transformations and relative content fluctuations were compared with each other to clarify the material basis transformations brought about by solid-state fermentation. Finally, based on the summarized chemical transformations, the antioxidant activities of SF-AP and Astragali radix were also evaluated. The general procedures of the strategy were summarized into a diagram in Fig. 1.

3.2. The characterization of chemical constituents

Structural elucidation was performed on the basis of chromatographic retention behaviors, accurate mass measurements, mass fragmentation patterns, DPIs and previous relevant literature. It should be noted that DPIs were significant to rapidly perform the structural elucidation, which were produced in by the comparable fragmentation patterns of the constituents with similar backbone (Zhao et al., 2018a,2018b). Finally, a total of 114 chemical constituents including 45 triterpene saponins (Table 1) and 69 flavonoids (Table 2) were accurately or tentatively characterized.

3.2.1. Structural identification of triterpenoid saponins in SF-AP and Astragali radix

Saponins are important effective components existing in Astragali radix, most of which are tetracyclic triterpenoids. Based on the retention time, ESI-MS and ESI-MS/MS data, a total of 45 constituents attributed to triterpene saponins were screened

and identified from SF-AP sample and Astragali radix. These constituents mostly belong to cycloartane-type triterpenoids, which were mainly derivatives of 9, 19-cyclolanostane cycloastragenol or 9, 19-cyclolanostane cyclocanthogenin, 9, 10-secocycloartane and oleanane-type triterpenoid saponins (Chu et al., 2010).

In addition, Astragaloside I and Astragaloside IV were selected as subjects to determine their DPIs for the subsequent structural identification. Both reference standards possessed the same backbone structure while the quantity of acetyl groups connected to xylose were different. There are two acetyl groups at 2 and 3 position of xylose in Astragaloside I, while zero acetyl group in Astragaloside IV. Owing to the special structure of acetyl group (Ac), Astragaloside I could generate some characteristic fragment ions by loss of Ac (42 Da), Ac + H₂O (60 Da) and 2Ac (84 Da). Moreover, by comparing with the characteristic dissociation pathways in the MS/MS spectra of the other reference standards, some DPIs of triterpene saponins could be summarized in Fig. 2, which provided a basis for further characterization of the others candidates. Taking negative ion mode as an example, the mass spectrometry cleavage of triterpene saponins usually lose glucose (Glc, 162 Da), xylose (Xyl, 132 Da), H₂O (18 Da), CO₂ (44 Da), malonyl (Ma, 86 Da) and acetyl group (Ac, 42 Da) to generate the corresponding DPIs.

A7, A8 and A11 all possessed the [M-H]⁻ ions at *m/z* 785.46983 (C₄₁H₆₉O₁₄, mass error within ± 5 ppm). In their ESI-MS² spectra, they could yield a wide range of DPIs just like [M-H-Glc-Xyl]⁻ ion at *m/z* 491, [M-H-Glc]⁻ ion at *m/z* 623, [M-H-Xyl]⁻ ion at *m/z* 653, [M-H-H₂O]⁻ ion at *m/z* 767, and [M-H-CO₂]⁻ ion at *m/z* 741. Hence, A7, A8 and A11 were tentatively judged as Cyclocanthoside E or its isomers.

A10, A31 and A33 showed the identical [M-H]⁻ ions at *m/z* 813.46474 (C₄₂H₆₉O₁₅, mass error within ± 5 ppm). In the ESI-MS² spectra, a number of DPIs such as *m/z* 651 [M-H-Glc]⁻, *m/z* 633 [M-H-Glc-H₂O]⁻, *m/z* 795 [M-H-H₂O]⁻ and *m/z* 767 [M-H-H₂O-CO]⁻ were all observed. Meanwhile, combined with the bibliography data and fragmentation pathways, A10, A31 and A33 were tentatively characterized as Astramembranoside A or its isomers.

A13, A17, A26 and A29 all possessed the [M-H]⁻ ions at *m/z* 825.46419 (C₄₃H₆₉O₁₅, mass error within ± 5 ppm). Owing to the successive loss of acetyl, acetyl + H₂O and xylose + acetyl + H₂O, the [M-H]⁻ ion generated a serial of DPIs at *m/z* 783, *m/z* 765 and *m/z* 633 in the ESI-MS² spectra. Based upon the comparison of ESI-MS/MS spectra and retention

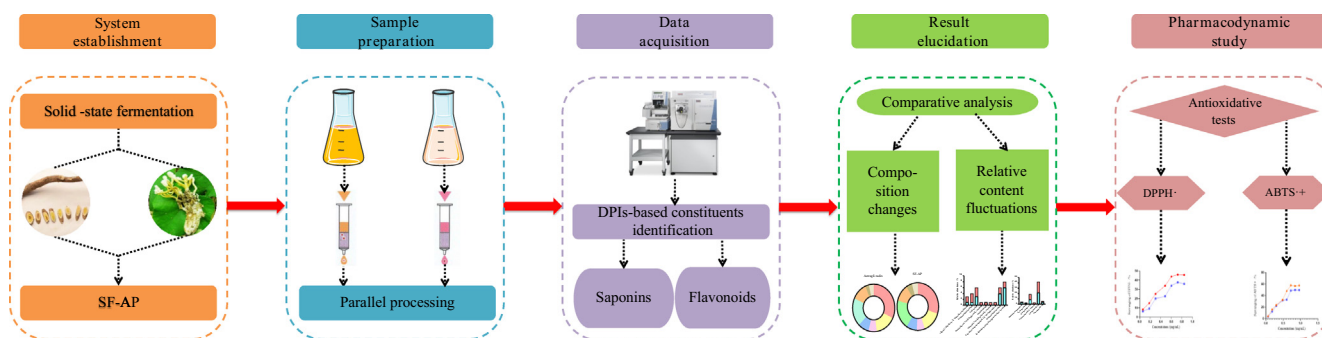


Fig. 1 The summary diagram of analytical strategy and methodology.

Table 1 Identification of saponins in Astragali radix and SF-AP.

Peak	t _R /min	Ion mode	Formula	Theoretical Mass <i>m/z</i>	Experimental Mass <i>m/z</i>	Error (ppm)	MS/MS fragment ions	Identification	A	S
A1	7.57	P	C ₄₈ H ₇₉ O ₁₈	943.52664	943.52582	-0.288	MS ² [943]:925 (100),927(76),1399 (37),486(30),859 (13),927(13),845 (10),827(6)	Soyasaponin I/isomer	+	+
A2	9.32	P	C ₄₃ H ₇₁ O ₁₅	827.47875	827.47443	-4.218	MS ² [827]:709 (100),809(10),691 (9),768(4),737(2),695 (2),577(2),335(2),467(1)	Astragaloside II isomer	+	+
A3	9.80	P	C ₃₈ H ₆₃ O ₁₁	695.43704	695.43274	-4.391	MS ² [695]:577 (100),499(35),677 (25),514(10),559(7),605 (4),532(4),199(2)	Mongholicoside II isomer	+	+
A4	10.38	P	C ₃₈ H ₆₃ O ₁₁	695.43704	695.43274	-4.391	MS ² [695]:577 (100),677(12),519 (9),499(6),559(6),636 (4),578(4),605(3)	Mongholicoside II	+	+
A5*	10.75	N	C ₄₇ H ₇₇ O ₁₉	945.50700	945.50916	3.023	MS ² [945]:783 (100),489(3),621 (2),765(1),651(1)	Astragaloside V	+	+
		P	C ₄₇ H ₇₉ O ₁₉	947.52155	947.52026	-0.788	MS ² [947]:437 (100),455(58),419 (38),587(21),785 (16),473(14),599 (11),535(11),738 (10),472(10),277(10)			
A6	11.51	P	C ₄₉ H ₈₁ O ₁₈	957.54229	957.54187	0.134	MS ² [957]:776 (100),777(22),794 (19),644(12),335(9),795 (4),336(3),643(2),645 (2),353(1)	Azukisaponin V methyl ester	-	+
A7	11.61	N	C ₄₁ H ₆₉ O ₁₄	785.46983	785.47198	4.834	MS ² [785]:491 (100),623(26),415 (16),740(13),767 (11),367(10),489(8)	Cyclocanthoside E/isomer	+	+
A8	11.77	N	C ₄₁ H ₆₉ O ₁₄	785.46983	785.46277	-4.892	MS ² [785]:491 (100),829(55),830 (26),767(24),653(21)	Cyclocanthoside E/isomer	+	+
A9*	11.79	N	C ₄₁ H ₆₇ O ₁₄	783.45363	783.45612	1.578	MS ² [783]:489 (100),621(46),651 (36),383(15),737 (12),453(11),646 (11),515(8),471(6)	Isoastragaloside IV	+	+
A10	12.38	N	C ₄₂ H ₆₉ O ₁₅	813.46474	813.46729	4.154	MS ² [813]:767 (100),745(78),652 (47),651(30),489 (30),633(27),795(26)	Astramembranoside A	+	+
		P	C ₄₂ H ₇₁ O ₁₅	815.47930	815.47729	-1.788	MS ² [815]:554 (100),711(98),276 (97),252(96),250 (94),505(93),315 (92),806(89)			
A11	12.46	N	C ₄₁ H ₆₉ O ₁₄	785.46983	785.47180	4.605	MS ² [785]:491 (100),623(24),767 (13),741(4),653(4),701 (3)	Cyclocanthoside E/isomer	+	+
A12	12.51	P	C ₄₉ H ₈₁ O ₂₀	989.53212	989.53296	1.404	MS ² [989]:503 (100),827(99),599 (96),483(95),330 (94),584(94),344 (93),452(93),603(92)	Agroastragaloside IV	+	+

(continued on next page)

Table 1 (continued)

Peak	t _R / min	Ion mode	Formula	Theoretical Mass <i>m/z</i>	Experimental Mass <i>m/z</i>	Error (ppm)	MS/MS fragment ions	Identification	A	S
A13	12.59	N	C ₄₃ H ₆₉ O ₁₅	825.46419	825.46735	4.151	MS ² [8 2 5]:765 (100),783(45),757 (17),787(12),779 (11),788(5),673(5),401 (4)	Astragaloside II isomer	+	+
A14	13.19	N	C ₃₆ H ₆₁ O ₁₁	669.42248	669.42383	4.468	MS ² [6 6 9]:601 (100),632(62),654 (55),623(50),436 (42),541(41),651(21)	Mongholicoside A	+	+
A15	13.23	P	C ₄₀ H ₆₅ O ₁₂	737.44760	737.44507	-2.690	MS ² [7 3 7]:557 (100),691(23),689 (20),511(19),577 (18),509(12),673 (12),493(11),571(8),605 (7),677(7),529(6),475(4)	Huangqiyein F	-	+
A16	13.79	N	C ₄₃ H ₇₁ O ₁₅	827.48039	827.48138	3.181	MS ² [8 2 7]:759 (100),767(39),783 (36),757(34),781 (33),809(24),785 (22),770(20)	Agroastragaloside II isomer	+	+
A17 [#]	13.95	P	C ₄₃ H ₇₁ O ₁₅	827.47875	827.47742	-1.605	MS ² [8 2 7]:639 (100),558(98),232 (94),443(94),640 (91),294(90),579 (90),231(89),295 (83),371(83)	Isoastragaloside II	+	+
		N	C ₄₃ H ₆₉ O ₁₅	825.46419	825.46710	2.849	MS ² [8 2 5]:765 (100),783(63),644 (31),762(19)			
A18 [#]	14.31	P	C ₄₁ H ₆₉ O ₁₄	785.46818	785.46722	-1.226	MS ² [7 8 5]:782 (100),720(78),237 (74),575(74),526 (73),434(72),480 (72),248(70)	Astragaloside IV	+	+
		N	C ₄₁ H ₆₇ O ₁₄	783.45363	783.45813	2.144	MS ² [7 8 3]:621 (100),489(50),490 (31),651(23),708 (23),553(18),700 (17),471(14),			
A19	14.56	N	C ₄₁ H ₆₇ O ₁₄	783.45363	783.45654	4.115	MS ² [7 8 3]:489 (100),383(13),651 (12),453(4),401(2),471 (2),381(2),760(2)	Astragaloside III	+	+
A20	14.56	N	C ₄₁ H ₆₉ O ₁₄	785.46983	785.46246	-4.286	MS ² [7 8 5]:491 (100),489(53),385 (15),383(11),491 (11),622(11),718(5)	Isoastragaloside IV isomer	+	+
A21	16.01	P	C ₃₆ H ₅₉ O ₁₀	651.41082	651.40857	-2.616	MS ² [6 5 1]:177 (100),199(62),269 (44),234(42),180 (38),574(37),663 (37),379(36),229 (35),300(32)	Huangqiyein A	-	+
A22	16.10	N	C ₅₁ H ₈₁ O ₂₁	1029.52758	1029.52173	-4.619	MS ² [1029]:985 (100),984(18),967(2)	Agroastragaloside III	+	+
		P	C ₅₁ H ₈₃ O ₂₁	1031.54214	1031.54199	-0.141	MS ² [1031]:984 (100),494(57),558 (52),331(50),667 (49),936(48),323 (47),482(46),300(45)			

Table 1 (continued)

Peak	t _R / min	Ion mode	Formula	Theoretical Mass <i>m/z</i>	Experimental Mass <i>m/z</i>	Error (ppm)	MS/MS fragment ions	Identification	A	S
A23	16.23	N	C ₄₇ H ₇₃ O ₁₇	909.48532	909.48804	4.192	MS ² [909]:891 (100),613(99),523 (80),453(76),849 (61),569(58),435 (36),746(25),495(18)	Acetylastragaloside I/isomer	+	+
A24	16.29	N	C ₄₈ H ₇₇ O ₁₈	941.51209	941.50549	-4.259	MS ² [941]:922 (100),524(56),873 (36),923(32),615 (27),523(26),879 (20),456(18),	Soyasaponin I/isomer	+	+
A25	16.36	P	C ₄₂ H ₆₇ O ₁₄	795.45308	795.45203	-0.632	MS ² [795]:421 (100),597(86),214 (81),295(74),429 (74),512(72),233 (72),625(71)	Huangqiyein E	-	+
A26	16.71	N	C ₄₃ H ₆₉ O ₁₅	825.46419	825.46796	4.890	MS ² [825]:765 (100),633(30),744 (18),634(17),736 (11),717(9),536(8),703 (7)	Astragaloside II isomer	+	+
		P	C ₄₃ H ₇₁ O ₁₅	827.47875	827.47729	-1.762	MS ² [827]:269 (100),592(67),629 (66),351(64),296 (63),632(60),709 (60),247(59),277(57)			
A27	16.74	N	C ₃₆ H ₅₉ O ₁₁	667.40683	667.40820	4.512	MS ² [667]:649 (100),449(82),623 (81),299(80),450 (74),485(54)	Mongholicoside B	+	+
A28	16.84	N	C ₄₈ H ₇₇ O ₁₈	941.51209	941.51392	3.694	MS ² [941]:923 (100),525(73),615 (51),744(49),879 (41),457(40),795 (37),437(35),597(16)	Soyasaponin I/isomer	+	+
		P	C ₄₈ H ₇₉ O ₁₈	943.52664	943.52496	-1.200	MS ² [943]:599 (100),797(88),441 (79),423(48),617 (28),581(23),520 (10),269(8),454(8),867 (8),448(8)			
A29 [#]	16.91	N	C ₄₃ H ₆₉ O ₁₅	825.46419	825.46631	3.892	MS ² [825]:783 (100),765(49),633 (24),795(10),697(9),758 (7)	Astragaloside II	+	+
A30	17.25	N	C ₄₃ H ₇₁ O ₁₅	827.48039	827.48267	4.740	MS ² [827]:809 (100),757(69),781 (40),758(38),769 (25),783(20),767(19)	Agroastragaloside II	+	+
A31	17.53	N	C ₄₂ H ₆₉ O ₁₅	813.46474	813.46686	4.625	MS ² [813]:725 (100),455(43),633 (30),651(29),767 (28),523(25),407 (22),795(21)	Astramembranoside A	+	+
A32	18.80	N	C ₄₂ H ₆₅ O ₁₄	793.43853	793.44080	4.937	MS ² [793]:631 (100),775(24),663 (8),724(7),747(5),718 (5),697(4)	Huangqiyein E/isomer	+	+
A33	18.83	N	C ₄₂ H ₆₉ O ₁₅	813.46474	813.46692	4.699	MS ² [813]:745 (100),767(36),489 (20),729(18),726 (15),651(14),305(9)	Astramembranoside A	+	+

(continued on next page)

Table 1 (continued)

Peak	t _R / min	Ion mode	Formula	Theoretical Mass <i>m/z</i>	Experimental Mass <i>m/z</i>	Error (ppm)	MS/MS fragment ions	Identification	A	S
A34 [#]	18.94	N	C ₄₅ H ₇₁ O ₁₆	867.47476	867.47809	3.104	MS ² [8 6 7]:807 (100),821(63),765 (53),783(22),849 (21),687(17)	Isoastragaloside I	+	+
A35	19.16	N	C ₄₇ H ₇₃ O ₁₇	909.48532	909.48846	4.654	MS ² [9 0 9]:891 (100),849(48),763 (47),453(46),569 (29),523(27),613 (19),407(16)	Acetylastragaloside I/isomer	+	+
A36	19.21	N	C ₄₈ H ₇₇ O ₁₈	941.51209	941.50427	-4.555	MS ² [9 4 1]:922 (100),524(44),879 (37),614(36),523 (36),613(32),732(31)	Soyasaponin I	+	+
A37	19.27	P	C ₄₂ H ₆₇ O ₁₄	795.45308	795.45209	-0.557	MS ² [7 9 5]:439 (100),597(89),421 (44),600(43),528 (36),253(35),299 (33),245(31)	Huangqiyein E	+	+
A38	19.37	N	C ₄₅ H ₇₁ O ₁₆	867.47476	867.47766	4.608	MS ² [8 6 7]:821 (100),799(34),731 (23),717(16),343 (15),787(11),831(8)	Astragaloside I isomer	+	+
A39	20.15	N	C ₄₂ H ₆₅ O ₁₄	793.43853	793.44073	4.849	MS ² [7 9 3]:725 (100),455(43),631 (30),663(29),747 (28),775(21),689 (20),279(19),636 (14),588(13),753(11)	Huangqiyein E/isomer	+	+
A40	20.20	P	C ₃₆ H ₆₃ O ₁₁	671.43704	671.43341	-4.586	MS ² [6 7 1]:479 (100),461(33),478 (8),443(8),611(8),653 (6),177(4),417(3),460 (3),199(2)	Mongholicoside A	+	+
A41 [#]	20.37	N	C ₄₅ H ₇₁ O ₁₆	867.47476	867.47662	2.410	MS ² [8 6 7]:849 (100),799(85),783 (81),821(77),747 (39),687(33)	Astragaloside I	+	+
A42 [#]	20.92	N	C ₄₅ H ₇₁ O ₁₆	867.47476	867.47943	3.684	MS ² [8 6 7]:703 (100),747(80),599 (73),821(53),783 (44),799(35),807 (32),687(24)	β-D-Glucopyranoside, (3β,6α,16β,20R,24 s)-3-[(3,4- di-O-acetyl-β-D- xylopyranosyl)oxy]-20,24- epoxy-16,25-dihydroxy-9,19- cyclostan-6-yl	+	+
A43	22.12	N	C ₄₅ H ₇₃ O ₁₆	869.49096	869.49335	4.644	MS ² [8 6 9]:823 (100),851(46),599 (18),767(15),536 (11),809(10),749(8),705 (8)	Agroastragaloside I	+	+
A44	22.76	N	C ₄₇ H ₇₃ O ₁₇	909.48532	909.48846	4.654	MS ² [9 0 9]:849 (100),867(27),711 (10),453(8),891(7),803 (2)	Acetylastragaloside I/isomer	+	+
A45	22.77	P	C ₄₈ H ₇₅ O ₁₉	955.48853	955.48853	-1.231	MS ² [9 5 5]:742 (100),1884(96),478 (96),406(95),864 (95),561(94),701 (94),567(94),919(91)	Malonylastragaloside I	+	+
		N	C ₄₈ H ₇₃ O ₁₉	953.47570	953.47968	4.898	MS ² [9 5 3]:935 (100),5379(67),627 (40),891(23),469 (22),907(15),849(3),807 (14)			

[#]: Unambiguously identification by comparing with the reference substances; *: Structural validation by using the reference substances.
+ : detected; - : undetected; A: Astragal radix; S: SF-AP.

Table 2 Identification of flavanoids in Astragali radix and SF-AP.

Peak	t _R / min	Ion mode	Formula	Theoretical Mass <i>m/z</i>	Experimental Mass <i>m/z</i>	Error (ppm)	MS/MS fragment ions	Identification	A	S
B1	1.24	P	C ₂₃ H ₂₇ O ₁₀	463.16042	463.15952	-0.763	MS ² [4 6 3]:268(100),330(13),398(8),365(3),398(3),453(3),136(3)	Astraisoflavan-7-O-β-D-glucoside/isomer	-	+
B2[#]	1.54	P	C ₂₁ H ₂₁ O ₁₂	465.10330	465.09921	-4.617	MS ² [4 6 5]:429(100),303(59),398(23),314(23),285(21),363(18),199(17),366(17)	Isoquercitrin	+	+
B3	3.71	N	C ₂₃ H ₂₃ O ₁₁	475.12513	475.12048	-4.331	MS ² [4 7 5]:257(100),275(92),437(65),179(46),180(45),276(42),419(39),438(38),457(26),283(16)	Odoratin-7-O-β-D-glucoside/isomer	+	+
B4	3.98	P	C ₂₃ H ₂₇ O ₁₀	463.16042	463.15796	-4.131	MS ² [4 6 3]:205(100),415(93),266(68),267(36),378(33),433(32),301(27)	Astraisoflavan-7-O-β-D-glucoside/isomer	+	+
B5	4.37	N	C ₂₉ H ₃₇ O ₁₆	641.20926	641.21063	4.708	MS ² [6 4 1]:479(100),317(75),595(35),611(30),623(26),379(24),610(22)	5'-hydroxy isomucronulatol 2',5'-di-O-glucoside	+	+
B6	4.37	P	C ₂₄ H ₂₅ O ₁₂	505.13460	505.13318	-1.727	MS ² [5 0 5]:333(100),335(41),306(33),373(26),438(21),281(21),343(13),282(11),317(9),181(7),487(6)	Neocomplanoside/isomer	+	+
B7	4.76	N	C ₂₈ H ₃₁ O ₁₆	623.16231	623.16388	4.165	MS ² [6 2 3]:299(100),284(31),604(7),283(6),461(6),605(5),415(5),577(4)	Complanatuside isomer	+	+
B8	4.86	P	C ₂₃ H ₂₉ O ₁₀	465.17607	465.17184	-4.919	MS ² [4 6 5]:303(100)446(6),429(6),432(5),302(2),346(1),301(1)	Astraisoflavan-7-O-β-D-glucoside/isomer	+	+
B9[#]	5.23	N	C ₂₈ H ₃₁ O ₁₆	623.16231	623.16364	3.780	MS ² [6 2 3]:299(100),284(32),461(10),240(4),461(3),577(2),605(2),211(2),239(2)	Complanatuside	+	+
B10	5.37	N P	C ₂₂ H ₂₁ O ₁₁ C ₂₂ H ₂₃ O ₁₁	461.10948 463.12404	461.11050 463.12265	4.773 -1.809	MS ² [4 6 1]:299(100),284(9) MS ² [4 6 3]:445(100),371(29),253(19),285(19),344(4),401(3),301(3)	Kaempferol- 4'-methylether-3-D-glucoside	+	+
B11	5.53	P	C ₁₆ H ₁₇ O ₅	289.10760	289.10645	-2.076	MS ² [2 8 9]:271(100),205(91),270(68),233(41),207(16),261(15),231(13),247(10),163(8),219(7),184(7),177(6),229(5),213(5)	(3R)-7,2',3'-Trihydroxy-4'-methoxy isoflavonone/isomer	+	-
B12	5.92	P N	C ₁₆ H ₁₃ O ₅ C ₁₆ H ₁₁ O ₅	285.07630 283.06175	285.07529 283.06198	-1.614 4.642	MS ² [2 8 5]:270(100),253(43),225(19),137(8),229(7),257(3),181(2),271(1) MS ² [2 8 3]:268(100),269(3),255(1)	Calycosin isomer	+	- +
B13	6.19	N	C ₂₂ H ₂₁ O ₁₂	477.10440	477.10532	4.382	MS ² [4 7 7]:315(100),301(18),300(14),347(13),431(11),459(5),297(4)	Isorhamnetin-3-O-β-D-glucoside	+	+
B14	6.19	P	C ₂₂ H ₂₃ O ₁₀	447.12912	447.12695	-3.630	MS ² [4 4 7]:300(100),283(19),255(7),167(5),301(5),259(4),138(3),269(3),168(2),297(1)	Calycosin-7-O-β-D-glucoside isomer		
B15	6.19	N	C ₂₄ H ₂₃ O ₁₂	503.12005	503.12112	4.401	MS ² [5 0 3]:299(100),284(23),443(4),467(2),488(1),240(1)	Neocomplanoside/isomer	+	+
B16	6.21	P N	C ₁₆ H ₁₃ O ₅ C ₁₆ H ₁₁ O ₅	285.07630 283.06175	285.07526 283.06180	-1.719 4.006	MS ² [2 8 5]:270(100),253(42),225(18),137(8),229(6),271(4),257(3),181(2) MS ² [2 8 3]:268(100),269(5),239(2),265(1),255(1)	Calycosin isomer	+	+
B17	6.34	P	C ₁₇ H ₁₅ O ₆	315.08686	315.08603	-0.903	MS ² [3 1 5]:300(100),283(20),255(8),167(5),259(4),301(2),287(2),175(2)	7,3'-dihydroxy-8,4-dimethoxyisoflavone isomer	+	+

(continued on next page)

Table 2 (continued)

Peak	t _R / min	Ion mode	Formula	Theoretical Mass <i>m/z</i>	Experimental Mass <i>m/z</i>	Error (ppm)	MS/MS fragment ions	Identification	A	S
B18	6.34	P	C ₂₃ H ₂₅ O ₁₁	477.13969	477.13779	-2.825	MS ² [477]:458(100),356(98),398(41),361(26),305(14),459(11),289(8),357(7),445(7),333(7),287(6),272(5),169(5)	Odoratin-7-O-β-D-glucoside isomer	+	+
B19	6.35	N	C ₁₇ H ₁₃ O ₆	313.07231	313.07236	4.415	MS ² [313]:298(100),285(2),295(1),269(1),283(1)	7,3'-Dihydroxy-8,4-dimethoxyisoflavone/isomer	+	+
B20	6.72	N	C ₁₅ H ₉ O ₅	269.04610	269.04605	4.947	MS ² [269]:225(100),241(36),197(23),181(22),236(16),226(11),183(11),251(9),213(9),201(8),254(8)	5,7,4'-trihydroxy-isoflavonone/isomer	+	+
B21	7.00	N	C ₁₆ H ₁₁ O ₅	283.06175	283.06192	4.430	MS ² [283]:268(100),269(3),265(1),239(1)	Calycosin isomer	+	+
		P	C ₁₆ H ₁₃ O ₅	285.07630	285.07529	-1.614	MS ² [285]:270(100),253(43),225(20),285(17),137(9),229(7),286(4),257(3),181(2)			
B22	7.01	P	C ₁₆ H ₁₇ O ₅	289.10760	289.10651	-1.868	MS ² [289]:270(100),271(22),184(8),252(8),166(7),205(4),182(2)	(3R)-7,2',3'-trihydroxy-4'-methoxy isoflavonone/isomer	+	-
B23*	7.10	N	C ₂₂ H ₂₁ O ₁₀	445.11457	445.11575	3.351	MS ² [445]:283(100),268(17),255(9)	Calycosin-7-O-β-D-glucoside	+	+
B24	7.19	N	C ₁₇ H ₁₃ O ₆	313.07231	313.07230	4.224	MS ² [313]:298(100),181(17),245(8),137(6),295(6),269(5),285(5),194(3)	7,3'-dihydroxy-8,4-dimethoxyisoflavone/isomer	+	+
B25[#]	7.25	N	C ₂₁ H ₁₉ O ₁₀	431.09892	431.09961	2.421	MS ² [431]:268(100),269(48),311(8),162(6)	Genistin	+	+
B26	7.30	N	C ₂₄ H ₂₃ O ₁₁	487.12513	487.12631	4.793	MS ² [487]:193(100),178(15),161(13),179(11),323(10),163(8),355(5),203(5),293(4)	Calycosin-7-O-β-D-glucoside-6''-O-acetate/isomer	+	+
B27	7.35	N	C ₁₆ H ₁₁ O ₅	283.06175	283.06189	4.324	MS ² [283]:268(100),269(1)	Calycosin isomer	+	+
B28	7.37	P	C ₁₆ H ₁₃ O ₅	285.07630	285.07571	-0.140	MS ² [285]:270(100),253(43),225(20),255(14),137(8),229(7),268(5),257(3),181(2),197(1)	Calycosin isomer	+	+
B29	7.39	P	C ₁₇ H ₁₅ O ₆	315.08686	315.08575	-1.792	MS ² [315]:300(100),283(19),255(9),269(8),297(5),167(5),259(4),138(3)	Kumatakenin	+	+
B30	7.52	N	C ₂₃ H ₂₇ O ₁₀	463.16152	463.16220	4.023	MS ² [463]:301(100),283(40),273(37),191(36),341(11),176(9),268(3)	Astraisoflavan-7-O-β-D-glucoside/isomer	+	+
B31	7.69	P	C ₁₅ H ₁₁ O ₅	271.06065	271.05978	-1.180	MS ² [271]:151(100),250(78),251(12),66(8),252(7),215(7),153(6),243(5),256(5),137(4),253(4)	5,7,4'-trihydroxy-isoflavonone/isomer	+	-
B32	7.70	N	C ₂₄ H ₂₃ O ₁₁	487.12513	487.12631	4.793	MS ² [487]:283(100),268(50),427(14),193(11),419(10),253(3)	Calycosin-7-O-β-D-glucoside-6''-O-acetate	+	+
B33	7.88	N	C ₁₆ H ₁₁ O ₄	267.06683	267.06693	4.533	MS ² [267]:252(100),253(5),249(2)	Formononetin isomer	+	+
		P	C ₁₆ H ₁₃ O ₄	269.08138	269.08051	-1.209	MS ² [269]:254(100),237(51),213(35),253(13),107(9),118(6),241(6),136(5)			
B34	7.89	N	C ₁₅ H ₉ O ₅	269.04610	269.04617	4.393	MS ² [269]:225(100),254(88),241(78),201(64),181(53),197(43),180(38),223(30)	5,7,4'-trihydroxy-isoflavonone/isomer	+	+
		P	C ₁₅ H ₁₁ O ₅	271.06065	271.05972	-1.402	MS ² [271]:243(100),153(87),215(85),239(50),66(41),149(36),253(34),211(30),221(25),159(16),199(14)			
B35	7.93	N	C ₂₉ H ₃₇ O ₁₅	625.21434	625.21527	4.116	MS ² [625]:301(100),463(9),286(4),445(3),607(2),271(2),473(1)	Isomucronulatol-7,2'-di-O-glucoside	+	+

Table 2 (continued)

Peak	t _R /min	Ion mode	Formula	Theoretical Mass <i>m/z</i>	Experimental Mass <i>m/z</i>	Error (ppm)	MS/MS fragment ions	Identification	A	S
B36	7.99	P	C ₁₇ H ₁₇ O ₅	301.10760	301.10669	-1.196	MS ² [301]:167(100),284(66),269(54),241(19),191(19),147(17),267(10),163(9),245(9)	3,9-dimethoxy-10-hydroxypterocarpan/isomer	+	+
B37	8.12	N	C ₁₆ H ₁₁ O ₅	283.06175	283.06168	4.582	MS ² [283]:268(100),269(3),255(1)	Calycosin isomer	+	+
B38	8.15	P	C ₂₄ H ₂₅ O ₁₁	489.13969	489.13794	-2.449	MS ² [489]:285(100),177(5),471(5),387(4),470(4),471(3),294(3),443(2),371(2)	Calycosin-7-O-β-D-glucoside-6''-O-acetate/isomer	+	+
B39	8.24	N	C ₁₆ H ₁₁ O ₄	267.06683	267.06702	4.870	MS ² [267]:252(100),253(1)	Formononetin isomer	+	+
B40	8.24	N	C ₂₃ H ₂₃ O ₁₁	475.12513	475.12625	4.813	MS ² [475]:267(100),456(1),252(1)	Odoratin-7-O-β-D-glucoside/isomer	+	+
B41 [#]	8.26	P	C ₂₂ H ₂₃ O ₉	431.13421	431.13263	-2.386	MS ² [431]:269(100),343(0.3),413(0.2)	Ononin	+	+
B42	8.27	P	C ₁₆ H ₁₃ O ₄	269.08138	269.08038	-1.692	MS ² [269]:254(100),237(51),213(40),241(17),66(14),252(12)	Formononetin isomer	+	+
B43	8.27	P	C ₂₆ H ₂₇ O ₁₁	515.15534	515.15076	-4.819	MS ² [515]:339(100),321(3),497(2),199(1)	Calycosin-7-O-β-D-glucoside-6''-O-butylene ester/isomer	+	-
B44	8.43	N	C ₁₇ H ₁₅ O ₅	299.09305	299.09293	4.115	MS ² [299]:284(100),269(1),255(1)	3,9-dimethoxy-10-hydroxypterocarpan/isomer	+	+
		P	C ₁₇ H ₁₇ O ₅	301.10760	301.10641	-2.126	MS ² [301]:167(100),269(26),191(21),147(19),163(12),273(11),207(9),286(6),241(6),270(3)			
B45	8.49	N	C ₁₆ H ₁₅ O ₅	287.09305	287.09317	4.165	MS ² [287]:135(100),272(91),165(46),177(29),121(22),147(19)	(3R)-7,2',3'-trihydroxy-4'-methoxy isoflavonone	+	+
B46	8.49	N	C ₂₉ H ₃₇ O ₁₅	625.21434	625.21716	4.139	MS ² [625]:323(100),367(71),324(70),343(48),325(36),445(26),547(24),366(17)	Isomucronulatol-7,2'-di-O-glucoside/isomer	+	+
B47	8.70	N	C ₂₉ H ₃₇ O ₁₅	625.21434	625.21558	-4.782	MS ² [625]:323(100),301(30),245(5),263(3),268(3),283(3),341(2),607(2)	Isomucronulatol-7,2'-di-O-glucoside/isomer	+	+
B48	8.78	N	C ₁₆ H ₁₁ O ₄	267.06683	267.06683	4.158	MS ² [267]:252(100),253(3),249(2),223(1)	Formononetin isomer	+	+
B49	8.92	N	C ₁₇ H ₁₅ O ₅	299.09305	299.09314	4.817	MS ² [299]:284(100),269(4)	3,9-dimethoxy-10-hydroxypterocarpan/isomer	+	+
		P	C ₁₇ H ₁₇ O ₅	301.10760	301.10641	-2.126	MS ² [301]:167(100),269(22),191(20),147(15),163(10),273(9),207(7),241(6),286(2),270(2)			
B50	9.02	N	C ₁₇ H ₁₇ O ₅	301.10870	301.10870	4.479	MS ² [301]:286(100),109(14),135(12),147(10),283(8),271(6),179(3)	(3R)-8,2'-dihydroxy-7,4'-dimethoxy-isoflavan/isomer	+	+
		P	C ₁₇ H ₁₉ O ₅	303.12325	303.12225	-1.485	MS ² [303]:167(100),149(32),123(19),284(16),181(14),168(7),219(6),270(5),193(5)			
B51	9.13	P	C ₁₆ H ₁₃ O ₄	269.08138	269.08041	-1.581	MS ² [269]:269(100),252(51),237(28),213(22),270(21),253(7)	Formononetin isomer	+	+
B52	9.19	N	C ₁₆ H ₁₁ O ₄	267.06683	267.06680	4.046	MS ² [267]:252(100),253(5)	Formononetin isomer	+	+
		P	C ₁₆ H ₁₃ O ₄	269.08138	269.08023	-2.250	MS ² [269]:254(100),237(52),269(51),213(40),253(15),270(13),107(10),136(6)			
B53	9.23	N	C ₁₇ H ₁₇ O ₅	301.10870	301.10880	4.811	MS ² [301]:286(100),135(19),109(15),147(10),121(8),283(6),271(6),179(6)	(3R)-8,2'-dihydroxy-7,4'-dimethoxy-isoflavan/isomer	+	+
		P	C ₁₇ H ₁₉ O ₅	303.12325	303.12219	-1.683	MS ² [303]:167(100),149(29),123(22),181(16),193(6),285(2),219(1),168(1)			

(continued on next page)

Table 2 (continued)

Peak	t _R / min	Ion mode	Formula	Theoretical Mass <i>m/z</i>	Experimental Mass <i>m/z</i>	Error (ppm)	MS/MS fragment ions	Identification	A	S
B54[#]	9.23	N	C ₂₃ H ₂₇ O ₁₀	463.16152	463.16254	2.757	MS ² [46 3]:301(100),286(5),299(1)	Astraisoflavan-7-O-β-D-glucoside	+	+
B55	9.37	N	C ₁₇ H ₁₃ O ₅	297.07740	297.07748	4.823	MS ² [29 7]:282(100),283(4),279(3),267(2),253(2),254(1),167(1)	Afrosomin	+	+
		P	C ₁₇ H ₁₅ O ₅	299.09195	299.09119	-0.702	MS ² [29 9]:284(100),166(23),243(21),239(11),267(11),285(10),137(4)			
B56	9.44	P	C ₁₆ H ₁₃ O ₄	269.08138	269.08035	-1.804	MS ² [26 9]:269(100),254(75),237(39),213(31),270(17),252(11)	Formononetin isomer	+	+
B57[#]	9.60	N	C ₁₆ H ₁₁ O ₄	267.06683	267.06699	4.757	MS ² [26 7]:252(100),253(1)	Calycosin	+	+
		N	C ₁₆ H ₁₁ O ₅	283.06175	283.06183	2.112	MS ² [28 3]:268(100),255(5)			
		P	C ₁₆ H ₁₃ O ₅	285.07630	285.07520	-1.929	MS ² [28 5]:270(100),253(43),225(20),137(9),229(7),257(3),181(2),175(1)			
B58	9.80	P	C ₁₇ H ₁₉ O ₅	303.12325	303.12247	-0.759	MS ² [30 3]:167(100),149(30),123(28),181(19),193(6)	(3R)-8,2'-dihydroxy-7,4'-dimethoxy-isoflavan/isomer	+	+
		N	C ₁₇ H ₁₇ O ₅	301.10870	301.10886	4.011	MS ² [30 1]:286(100),109(17),135(12),147(8),271(7),283(7),259(3),121(3)			
B59	9.98	N	C ₁₇ H ₁₅ O ₅	299.09305	299.09329	4.319	MS ² [29 9]:284(100),269(4)	3,9-dimethoxy-10-hydroxypterocarpan	+	+
		P	C ₁₇ H ₁₇ O ₅	301.10760	301.10657	-1.594	MS ² [30 1]:167(100),269(22),191(20),147(16),163(10),273(10),207(7),241(6),270(3)			
B60	10.00	P	C ₁₇ H ₁₅ O ₆	315.08686	315.08588	-1.379	MS ² [31 5]:300(100),283(19),138(11),255(5),186(7),168(7),294(5),167(5),259(4),296(3)	Kumatakenin	+	+
B61	10.01	N	C ₁₅ H ₉ O ₅	269.04610	269.04617	4.393	MS ² [26 9]:241(100),225(20),213(17),123(9),251(8),145(6),197(5)	5,7,4'-trihydroxy-isoflavanone	+	+
B62	10.25	N	C ₁₇ H ₁₅ O ₅	299.09305	299.09323	4.118	MS ² [29 9]:284(100),269(6),267(6),165(4),271(4),281(2)	3,9-dimethoxy-10-hydroxypterocarpan/isomer	+	+
B63	10.34	P	C ₂₆ H ₂₇ O ₁₁	515.15534	515.15393	-1.666	MS ² [51 5]:411(100),353(19),497(13),455(13),393(10),369(10),597(10),337(9),335(8),395(7),167(6)	Calycosin-7-O-β-D-glucoside-6''-O-butylene ester/isomer	+	+
B64	10.38	N	C ₁₇ H ₁₇ O ₅	301.10870	301.10886	4.011	MS ² [30 1]:286(100),135(38),121(17),109(13),147(10),283(8),179(7),271(6)	(3R)-8,2'-dihydroxy-7,4'-dimethoxy-isoflavan/isomer	+	+
		P	C ₁₇ H ₁₉ O ₅	303.12325	303.12247	-0.759	MS ² [30 3]:167(100),149(29),123(23),181(16),193(7),285(2),261(1),167(1)			
B65	10.99	N	C ₁₆ H ₁₁ O ₄	267.06683	267.06693	4.533	MS ² [26 7]:252(100),253(5),249(2)	Formononetin isomer	+	+
B66	11.75	P	C ₁₇ H ₁₇ O ₅	301.10760	301.10690	-0.499	MS ² [30 1]:167(100),269(22),191(20),147(16),163(10),281(10),207(7),241(6),267(4)	3,9-dimethoxy-10-hydroxypterocarpan/isomer	+	+
B67[#]	14.00	N	C ₁₆ H ₁₁ O ₄	267.06683	267.06699	2.757	MS ² [26 7]:252(100),253(3)	Formononetin	+	+
		P	C ₁₇ H ₁₃ O ₅	269.08138	269.08041	-1.581	MS ² [26 9]:254(100),237(45),251(36),213(26),253(14),107(10),118(5)			
B68	14.69	P	C ₁₇ H ₁₇ O ₅	301.10760	301.10666	-1.296	MS ² [30 1]:167(100),269(81),147(46),191(45),163(28),273(24),267(20),241(18),281(7),270(6),284(4)	3,9-dimethoxy-10-hydroxypterocarpan/isomer	+	+
B69	15.28	P	C ₁₇ H ₁₉ O ₅	303.12325	303.12262	-0.264	MS ² [30 3]:167(100),149(33),123(22),181(15),193(7),280(7),199(2)	(3R)-8,2'-dihydroxy-7,4'-dimethoxy-isoflavan	+	+

[#]: Unambiguously identification by comparing with the reference substances; *: Structural validation by using the reference substances; +: detected; -: undetected; A: Astragal radix; S: SF-AP.

Structures		DPIs	
9,19-cyclolanostane cycloastragenol		A5: R ₁ =R ₄ =R ₅ =H R ₂ =R ₃ =Glc	[M-H-Xyl] ⁻ [M-H-Glc×n] ⁻ [M-H-Glc] ⁻ [M-H-Glc-Xyl] ⁻ [M-H-H ₂ O] ⁻ [M-H-H ₂ O×n] ⁻ [M-H-Ac] ⁻ [M-H-Ac×n] ⁻ [M-H-Glc-H ₂ O] ⁻ [M-H-Ac-H ₂ O] ⁻ [M-H-Glc-Ac-H ₂ O] ⁻
		A9: R ₁ =R ₃ =R ₄ =R ₅ =H R ₂ =Glc	
		A12: R ₁ =R ₂ =Glc R ₄ =R ₅ =H R ₃ =Ac	
		A17: R ₁ =Glc R ₂ =R ₃ =R ₅ =H R ₄ =Ac	
		A18: R ₁ =Glc R ₂ =R ₃ =R ₄ =R ₅ =H	
		A19: R ₁ =R ₂ =R ₄ =R ₅ =H R ₃ =Glc	
		A22: R ₁ =R ₂ =Glc R ₃ =R ₄ =Ac R ₅ =H	
		A23/A35/A44: R ₁ =Glc R ₂ =H R ₃ =R ₄ =R ₅ =Ac	
		A29: R ₁ =Glc R ₂ =R ₄ =R ₅ =H R ₃ =Ac	
		A34: R ₁ =Glc R ₂ =R ₄ =H R ₃ =R ₅ =Ac	
A41: R ₁ =Glc R ₂ =R ₅ =H R ₃ =R ₄ =Ac			
A45: R ₁ =Glc R ₂ =H R ₃ =R ₄ =Ac R ₅ =Malonyl			
9,19-cyclolanostane cycloanthogenin		A10: R ₁ =H R ₂ =α-O-Glc β-H R ₃ =Glc	[M-H-CO] ⁻ [M-H-H ₂ O] ⁻ [M-H-H ₂ O-CO] ⁻ [M-H-Glc] ⁻ [M-H-H ₂ O-Glc] ⁻
		A21*: R ₁ =Glc R ₂ =O β-H R ₃ =H	
9,19-cyclolanostane cycloanthogenin		A4: R ₁ =COCH ₃ R ₂ =OH R ₃ =Glc	[M-H-H ₂ O] ⁻ [M-H-CH ₃] ⁻ [M-H-H ₂ O-CH ₃] ⁻ [M-H-Glc] ⁻ [M-H-H ₂ O-Glc] ⁻ [M-H-CH ₃ -Glc] ⁻
		A7/A8/A11/A25*: R ₁ =R ₂ =R ₃ =H R ₄ =Glc	[M-H-Ac] ⁻ [M-H-Ac×n] ⁻ [M-H-H ₂ O] ⁻ [M-H-Glc] ⁻ [M-H-H ₂ O-Ac] ⁻ [M-H-Glc-AcH ₂ O] ⁻
		A30: R ₁ =Ac R ₂ =R ₃ =H R ₄ =Glc	
A43: R ₁ =R ₂ =Ac R ₃ =OH R ₄ =Glc			
9,10-seccycloartane triterpenoid saponons		A14: R ₁ =Glc R ₂ =α-OH β-H R ₃ =OH	[M-H-Glc] ⁻ [M-H-Glc-H ₂ O] ⁻ [M-H-H ₂ O] ⁻ [M-H-H ₂ O×n] ⁻
		A27: R ₁ =Glc R ₂ =O R ₃ =OH	
9,10-seccycloartane triterpenoid saponons		A15*: R=H	[M-H-Ac] ⁻ [M-H-Ac×n] ⁻ [M-H-H ₂ O] ⁻ [M-H-Glc] ⁻ [M-H-H ₂ O-Ac] ⁻
		A37: R=OAc	
Oleanane-type triterpenoid		A6*: R ₁ =OH R ₂ =H R ₃ =CH ₂ OH R ₄ =CH ₃	[M-H-CO ₂] ⁻ [M-H-H ₂ O] ⁻ [M-H-H ₂ O-CO ₂] ⁻ [M-H-GluA-Gal-Rha] ⁻
A36: R ₁ =R ₄ =H R ₂ =OH R ₃ =CH ₂ OH			

*: Detection after fermentation

Fig. 2 The summary structures and DPIs for the triterpenoid saponins in SF-AP and Astragali radix.

time with the corresponding reference standards, **A29** was positively identified as Astragaloside II, while **A17** was unambiguously characterized as Isoastragaloside II. The accurate mass weight and major product ions of **A13** and **A26** were broadly similar to those of **A29** and **A17**, which indicated that **A13** and **A26** could be deduced as the isomers of Astragaloside II or Isoastragaloside II.

A14 afforded $[M-H]^-$ ion at m/z 669.42248 ($C_{36}H_{61}O_{11}$) with mass error of 4.47 ppm. Due to the loss of H_2O (18 Da), $2H_2O$ (36 Da) and glucose (162 Da), the product ions in its ESI-MS² spectrum at m/z 651, m/z 633 and m/z 507 were respectively yielded. Therefore, according to the fragmentation pathways and literature data (Wang et al., 2019a), **A14** could be deduced as Mongholicoside A.

A23, **A35** and **A44** all afforded the $[M-H]^-$ ions at m/z 909.48532 ($C_{47}H_{73}O_{17}$, mass error within ± 5 ppm). In the MS/MS spectra, there were some product ions such as $[M-H-H_2O]^-$ at m/z 891, $[M-H-Ac-H_2O]^-$ at m/z 849 and m/z 453 $[M-H-3Ac-Xyl-Glc-2H_2O]^-$ at m/z 453. And thus, **A23**, **A35** and **A44** were tentatively characterized as Acetylasragaloside I or its isomers.

Both **A32** and **A39** provided the deprotonated $[M-H]^-$ ions at m/z 793.43853 ($C_{42}H_{65}O_{14}$, mass error within ± 5 ppm). The characteristic product ions such as $[M-H-Glc]^-$ ion at m/z 631, $[M-H-H_2O]^-$ ion at m/z 775 and $[M-H-2Ac-H_2O-CO]^-$ ion at m/z 663 were all illustrated in the ESI-MS² spectra. Hence, **A32** and **A39** were deduced to be Huangqiyein E or its isomer.

A34, **A38**, **A41** and **A42** gave the identical $[M-H]^-$ ions at m/z 867.47476 ($C_{45}H_{71}O_{16}$, mass error within ± 5 ppm). Based upon the obtained high-resolution mass spectrometry data, they yielded the DPIs at m/z 849, m/z 807, m/z 783, m/z 747 and m/z 687 by the respective loss of H_2O (18 Da), acetyl + H_2O (60 Da), 2acetyl (84 Da), 2acetyl + $2H_2O$ (120 Da) and glucose + H_2O (180 Da) in the ESI-MS² spectra. Compared with the standard substances, **A41** was identified as Astragaloside I and **A34** was characterized as Isoastragaloside I, while **A38** was characterized as Isoastragaloside I isomer. Moreover, **A42** was deduced as β -D-Glucopyranoside-(3 β , 6 α , 16 β , 20R, 24 s)-3-[(3, 4-di-O-acetyl- β -D-xylopyranosyl)oxy]-20, 24-epoxy-16, 25-dihydroxy-9, 19-cyclolanostan-6-yl.

A43 possessed the $[M-H]^-$ ion at m/z 869.49096 ($C_{45}H_{73}O_{16}$, mass error of 4.644 ppm). In the ESI-MS² spectrum, it yielded some DPIs at m/z 851, m/z 809, m/z 767 and m/z 749 through the successive loss of H_2O , acetyl + H_2O , 2acetyl + H_2O and 2acetyl + $2H_2O$, respectively. Hence, **A43** was tentatively interpreted as Agroastragaloside I.

A45 generated its $[M-H]^-$ ion at m/z 953.47570 ($C_{48}H_{73}O_{19}$) with mass error of 4.898 ppm. It further produced a series of fragment ions at m/z 935 $[M-H-H_2O]^-$, m/z 627 $[M-H-Glc-Ma-Ac-2H_2O]^-$, m/z 891 $[M-H-CO_2-H_2O]^-$, and m/z 807 $[M-H-Ma-Ac-H_2O]^-$ in its ESI-MS² spectrum. Therefore, **A45** was tentatively interpreted as Malonylastragaloside I. In addition, the ESI-MS² spectra of **A9**, **A17**, **A44** and **A45** were illustrated in Fig. 3.

In order to verify the fragmentation regularities, the other two reference substances were conducted. Take Astragaloside V and Isoastragaloside IV as examples, which would make structural validation clear. Based on the obtained high-resolution mass spectrometry data, it could be seen that Astragaloside V (**A5***) produced the $[M-H]^-$ ion at m/z 945.50700 ($C_{47}H_{77}O_{19}$). Then the $[M-H]^-$ ion generated a series of char-

acteristic product ions at m/z 783 $[M-H-Glc]^-$, m/z 651 $[M-H-Glc-Xyl]^-$, m/z 621 $[M-H-2Glc]^-$ and m/z 489 $[M-H-Xyl-2Glc]^-$ in its ESI-MS² spectrum. Isoastragaloside IV (**A9***) gave rise to $[M-H]^-$ ion at m/z 783.45363 ($C_{41}H_{67}O_{14}$). In its ESI-MS² spectrum, the $[M-H]^-$ ion at m/z 783 further generated several product ions at m/z 489, m/z 651, m/z 621, m/z 471, and m/z 453 by the subsequent losing xylose + glucose, xylose moiety, glucose moiety, xylose + glucose + H_2O , and xylose + glucose + $2H_2O$. By referring to the cracking mode of these two reference substances, some similar rules in cracking could be found. For the special structures of flavonoid glycoside, the ions of $[M-H-162]^-$ and $[M-H-132]^-$ were usually produced via the loss of glucose moiety and xylose moiety in their ESI-MS² spectra.

3.2.2. Structural identification of flavonoids in SF-AP and Astragali radix

Flavonoids are the other major category of components existing in Astragali radix. The DPIs for flavonoids have previously summarized on the basis of high-resolution MS data acquired in Fig. 4. The characteristic DPIs just like $[M-H-CH_3]^-$ (15 Da), $[M-H-H_2O]^-$ (18 Da), $[M-H-CO_2]^-$ (44 Da) and $[M-H-CO]^-$ (28 Da) were obviously observed according to the ESI-MS/MS data of the obtained reference standards. Meanwhile, flavonoid glycosides usually first split up the glycosidic bond, and then produce the corresponding aglycone ions (Ren et al., 2007; Es-Safi et al., 2007). Generally speaking, the glucose group is usually replaced at the C-7 or C-3 position of the ligand ketone. Subsequently, the aglycone ions would be cleaved to form a series of fragment ion. In addition, they will ordinarily lose Glc + H_2O + CO (208 Da) and Glc + CO + H_2O + CH_3 (223 Da). For polymethoxylated flavones, the fragment ions produced by loss of one or more methyl radicals from the protonated molecule ions are usually detected, which could be regarded as their DPIs (Zhang et al., 2011; Shang et al., 2017). Finally, 64 flavonoids including 33 isoflavones, 15 isoflavans, 7 pterocarpan and 9 flavones were identified from SF-AP while 69 flavonoids including 35 isoflavones, 18 isoflavans, 7 pterocarpan and 9 flavones were characterized from Astragali radix.

Both **B3** and **B40** yielded $[M-H]^-$ ions at m/z 475.12513 ($C_{23}H_{23}O_{11}$, mass error within ± 5 ppm). In the ESI-MS² spectra, a number of DPIs were observed such as m/z 267 $[M-H-Glc-H_2O-CO]^-$, m/z 252 $[M-H-Glc-CO-H_2O-CH_3]^-$ and m/z 429 $[M-H-H_2O-CO]^-$. Based on this, **B3** and **B40** were tentatively characterized as Odoratin-7-O- β -D-glucoside or its isomer.

B5 possessed the $[M-H]^-$ ion at m/z 641.20926 ($C_{29}H_{37}O_{16}$) with mass error of 4.708 ppm. Due to the presence of ESI-MS² product ions at m/z 479, m/z 317, m/z 433 and m/z 611 by losing glucose, 2glucose, CO + H_2O and $2CH_3$, **B5** was finally characterized as 5'-hydroxy-isomucronulatol-2', 5'-di-O-glucoside.

Both **B7** and **B9** generated the same $[M-H]^-$ ions at m/z 623.16231 ($C_{28}H_{31}O_{16}$, mass error within ± 5 ppm). Moreover, a range of characteristic DPIs at m/z 415 $[M-H-Glc-CO-H_2O]^-$, m/z 461 $[M-H-Glc]^-$, m/z 299 $[M-H-2Glc]^-$ and m/z 577 $[M-H-CO-H_2O]^-$ were detected in the ESI-MS/MS spectra. As a result, **B9** was tentatively characterized as Complanatuside, while **B7** was judged as Complanatuside isomer.

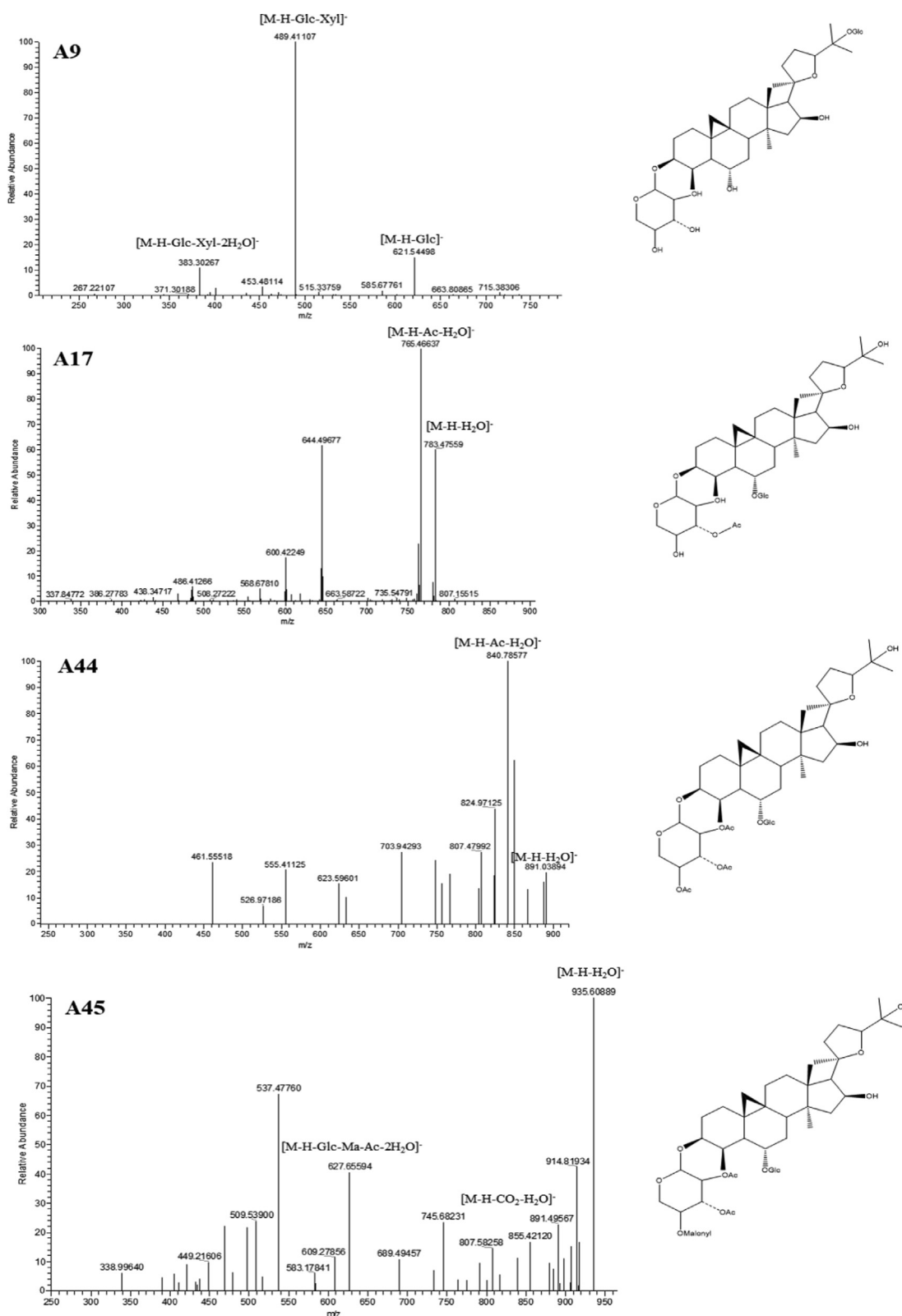
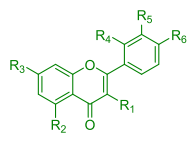
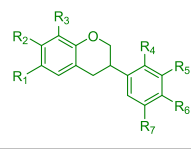
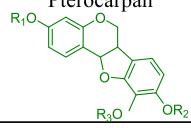
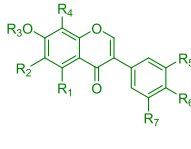


Fig. 3 The ESI-MS² spectra and chemical structures of **A9**, **A17**, **A44** and **A45**.

B10 gave rise to the $[M-H]^-$ ion at m/z 461.10948 ($C_{22}H_{21}O_{11}$) with mass error of 4.773 ppm. Based on the obtained high-resolution mass spectrometry data, it yielded respective base peak ions at m/z 446 $[M-H-CH_3]^-$, m/z 299

$[M-H-Glc]^-$, m/z 267 $[M-H-Glc-CH_2-H_2O]^-$ and m/z 271 $[M-H-Glc-CO]^-$ in the ESI-MS² spectra. Therefore, according to the fragmentation pathways, **B10** was characterized as Kaempferol-4'-methylether-3-D-glucoside.

Structures	DPIs
<p>Flavone</p>  <p>B2: R₁=O-Glc R₂=R₃=R₅=R₆=OH R₄=H B6/B15: R₁=O-(6-O-acetyl)-Glc R₂=R₆=OH R₃=OCH₃ R₄=R₅=H B9: R₁=R₆=O-Glc R₂=OH R₃=OCH₃ R₄=R₅=H B10: R₁=O-Glc R₂=R₃=OH R₄=R₅=H R₆=OCH₃ B13: R₁=O-Glc R₂=R₃=R₆=OH R₄=H R₅=OCH₃ B29: R₁=R₃=OCH₃ R₂=R₆=OH R₄=R₅=H</p>	<p>Methoxylated flavones</p> <ul style="list-style-type: none"> [M-H-CH₃]⁻ [M-H-CH₃×n]⁻ [M-H-H₂O]⁻ [M-H-CO]⁻ [M-H-H₂O-CH₃]⁻ [M-H-CO-CH₃]⁻ [M-H-H₂O-CO-CH₃]⁻ <p>Flavonoid glycosides</p> <ul style="list-style-type: none"> [M-H-Glc]⁻ [M-H-Glc×n]⁻ [M-H-H₂O]⁻ [M-H-CO]⁻ [M-H-H₂O-CO]⁻ [M-H-Glc-CO]⁻ [M-H-Glc-H₂O]⁻ [M-H-Glc-H₂O-CO]⁻
<p>Isoflavan</p>  <p>B5: R₁=R₃=H R₂=OH R₄=R₇=O-Glc R₅=R₆=OCH₃ B35: R₁=R₃=R₇=H R₂=R₄=O-Glc R₅=R₆=OCH₃ B11*/B22*/B45: R₁=R₃=R₇=H R₂=R₄=R₅=OH R₆=OCH₃ B54: R₁=R₃=R₇=H R₂=O-Glc R₄=OH R₅=R₆=OCH₃ B1*/B69: R₁=R₃=R₇=H R₂=R₆=OCH₃ R₃=R₄=OH</p>	<p>Methoxylated isoflavan</p> <ul style="list-style-type: none"> [M-H-CH₃]⁻ [M-H-CH₃×n]⁻ [M-H-H₂O]⁻ [M-H-H₂O-CH₃]⁻ <p>Flavonoid isoflavan</p> <ul style="list-style-type: none"> [M-H-Glc]⁻ [M-H-Glc×n]⁻ [M-H-H₂O]⁻ [M-H-Glc-H₂O]⁻
<p>Pterocarpan</p>  <p>B59: R₁=R₂=CH₃ R₃=H</p>	<p>[M-H-CH₃]⁻ [M-H-CH₃×n]⁻</p>
<p>Isoflavnone</p>  <p>B3/B40: R₁=R₄=R₇=H R₂=R₆=OCH₃ R₃=O-Glc R₅=OH B23: R₁=R₂=R₄=R₇=H R₃=Glc R₅=OH R₆=OCH₃ B19/B24: R₁=R₂=R₃=R₇=H R₄=R₆=OCH₃ R₅=OH B25: R₁=R₆=OH R₂=R₄=R₅=R₇=H R₃=Glc B32: R₁=R₂=R₄=R₇=H R₃=6''-acetate-O-Glc R₅=OH R₆=OCH₃ B41: R₁=R₂=R₄=R₅=R₇=H R₃=Glc R₆=OCH₃ B43*/B63: R₁=R₂=R₄=R₇=H R₃=6''-butylene ester-O-Glc R₅=OH R₆=OCH₃ B55: R₁=R₃=R₄=R₅=R₇=H R₂=R₆=OCH₃ B57: R₁=R₂=R₃=R₄=R₇=H R₅=OH R₆=OCH₃ B31*/B61: R₁=R₆=OH R₂=R₃=R₄=R₅=R₇=H B67: R₁=R₂=R₃=R₄=R₅=R₇=H R₆=OCH₃</p>	<p>Methoxylated isoflavones</p> <ul style="list-style-type: none"> [M-H-CH₃]⁻ [M-H-CH₃×n]⁻ [M-H-H₂O]⁻ [M-H-CO]⁻ [M-H-H₂O-CH₃]⁻ [M-H-CO-CH₃]⁻ [M-H-H₂O-CO-CH₃]⁻ <p>Flavonoid isoglycosides</p> <ul style="list-style-type: none"> [M-H-Glc]⁻ [M-H-Glc×n]⁻ [M-H-H₂O]⁻ [M-H-CO]⁻ [M-H-H₂O-CO]⁻ [M-H-Glc-CO]⁻ [M-H-Glc-H₂O]⁻ [M-H-Glc-H₂O-CO]⁻

*: Detection after fermentation; **: Undetection after fermentation

Fig. 4 The summary structures and DPIs for the flavonoids in SF-AP and Astragali radix.

Six isomeric constituents, **B12**, **B16**, **B21**, **B27**, **B37** and **B57**, afforded the same theoretical [M-H]⁻ ions at *m/z* 283.06175 (C₁₆H₁₁O₅, mass error within ± 5 ppm), respectively. In the ESI-MS spectra, they showed the characteristic ESI-MS² product ions at *m/z* 268 and *m/z* 255 by loss of CH₃ (15 Da) and CO (28 Da). Combined with the standard substance, **B57** was unambiguously identified as Calycosin. Meanwhile, the other five constituents including **B12**, **B16**, **B21**, **B27** and **B37** were tentatively characterized as Calycosin isomers.

B13 possessed the [M-H]⁻ ion at *m/z* 477.10440 (C₂₂H₂₁O₁₂) with mass error of 4.382 ppm. In the ESI-MS² spectrum, it produced many DPIs just like [M-H-Glc]⁻ ion at *m/z* 315, [M-H-H₂O-CO]⁻ ion at *m/z* 431, [M-H-Glc-H₂O]⁻ ion at *m/z* 297, [M-H-Glc-CH₃]⁻ ion at *m/z* 300 and [M-H-H₂O]⁻ ion at *m/z* 459. Combined with the standard substance, **B13** was positively identified as Isorhamnetin-3-D-glucoside.

B15 afforded the [M-H]⁻ ion at *m/z* 503.12005 (C₂₄H₂₃O₁₂, mass error of 4.401 ppm). In the ESI-MS/MS spectrum, it showed the product ions at *m/z* 299 [M-H-acetyl-Glc]⁻, *m/z* 488 [M-H-CH₃]⁻ and *m/z* 467 [M-H-2H₂O]⁻. And thus, it indicated that **B15** could be characterized as Neocomplanoside or its isomer.

B19 and **B24** afforded the same [M-H]⁻ ions at *m/z* 313.07231 (C₁₇H₁₃O₆, mass error within ± 5 ppm). They further produced DPIs at *m/z* 298 ([M-H-CH₃]⁻), *m/z* 295 ([M-H-H₂O]⁻), *m/z* 285 ([M-H-CO]⁻) and *m/z* 269 ([M-H-CO₂]⁻) in the ESI-MS/MS spectra. Hence, according to the proposed fragmentation patterns, **B19** and **B24** could be assumed as 7,3'-dihydroxy-8,4-dimethoxyisoflavone or its isomer.

B20, **B34** and **B61** afforded the same [M-H]⁻ ions at *m/z* 269.04610 (C₁₅H₉O₅, mass error within ± 5 ppm), respectively. There were a battery of DPIs at *m/z* 254 ([M-H-CH₃]⁻), *m/z* 241 ([M-H-Glc-CO]⁻), *m/z* 225

([M-H-CO₂]⁻), *m/z* 197 ([M-H-CO-CO₂]⁻) and *m/z* 181 ([M-H-2CO₂]⁻) in the ESI-MS/MS spectra. Therefore, **B20**, **B34** and **B61** could be characterized as 5,7,4'-trihydroxy-isoflavone or its isomers.

B25 generated the [M-H]⁻ ion at *m/z* 431.09892 (C₂₁H₁₉O₁₀) with mass error of 2.421 ppm. In the ESI-MS² spectrum, it further possessed the product ions at *m/z* 269 by the loss of 162 Da (glucose). By Combining with the standard substance, **B25** was positively characterized as Genistin.

Seven constituents containing **B33**, **B39**, **B48**, **B52**, **B56**, **B65** and **B67**, which respectively afforded the same identical [M-H]⁻ ions at *m/z* 267.06683 (C₁₆H₁₁O₄, mass error within ± 5 ppm). In the ESI-MS/MS spectra, they further yielded the product ion at *m/z* 252 by the loss of CH₃ radical. Combined with the standard substance, **B67** was unambiguously identified as Formononetin, while **B33**, **B39**, **B48**, **B52**, **B56** and **B65** could be deduced as Formononetin isomers.

B45 afforded the [M-H]⁻ ion at *m/z* 287.09305 (C₁₆H₁₅O₅, mass error of 4.165 ppm). In the ESI-MS/MS spectrum, it further generated the product ions at *m/z* 272 [M-H-CH₃]⁻, *m/z* 269 [M-H-H₂O]⁻ and *m/z* 255 [M-H-CH₂-H₂O]⁻. Based upon this, **B45** was deduced to be (3R)-7,2',3'-trihydroxy-4'-methoxy isoflavone.

B50, **B53**, **B58** and **B64** all gave rise to the same [M-H]⁻ ions at *m/z* 301.10870 (C₁₇H₁₇O₅, mass error within ± 5 ppm), respectively. In the ESI-MS/MS spectra, the DPIs at *m/z* 286 ([M-H-CH₃]⁻), *m/z* 283 ([M-H-H₂O]⁻) and *m/z* 271 ([M-H-2CH₃]⁻) were all observed. Combined with the obtained fragmentation pathways, **B50**, **B53**, **B58** and **B64** were characterized as (3R)-8,2'-dihydroxy-7,4'-dimethoxy-isoflavan or its isomers.

Five isomeric constituents, including **B44**, **B49**, **B59**, **B62** and **B72**, produced the same [M-H]⁻ ions at *m/z* 299.09305 (C₁₇H₁₅O₅, mass error within ± 5 ppm), respectively. There were a series of DPIs at *m/z* 284 [M-H-CH₃]⁻, *m/z* 269 [M-H-2CH₃]⁻, *m/z* 267 [M-H-CH₂-H₂O]⁻ and *m/z* 281 [M-H-H₂O]⁻ in the ESI-MS² spectra. And thus, **B44**, **B49**, **B59**, **B62** and **B72** were tentatively characterized as 3,9-dimethoxy-10-hydroxypterocarpan or its isomers.

B54 gave rise to the identical [M-H]⁻ ion at *m/z* 463.16152 (C₂₃H₂₇O₁₀, mass error 2.757 ppm). In the ESI-MS/MS spectrum, it showed the characteristic product ions at *m/z* 301 and *m/z* 286 by the loss of 162 Da (glucose) and 177 Da (glucose + CH₃). Combined with the corresponding standard substance, **B54** was identified as Astraisoflavan-7-O-β-D-glucoside.

B55 afforded the [M-H]⁻ ion at *m/z* 297.07740 (C₁₇H₁₃O₅) with mass error of 4.823 ppm. In its ESI-MS² spectrum, it generated some characteristic product ions such as *m/z* 282, *m/z* 253, *m/z* 267 and *m/z* 279 through the successive loss of CH₃, CO₂, 2CH₃, H₂O, orderly. Based upon this, **B55** was concluded to be Afromosin isomer. In addition, the ESI-MSⁿ spectra of **B9**, **B23**, **B57** and **B61** were all illustrated in Fig. 5.

For the reference substance with flavonoid structure, Calycosin-7-O-β-D-glucoside (**B23***) yielded the [M-H]⁻ ion at *m/z* 445.11457 (C₂₂H₂₁O₁₀) with mass error of 3.351 ppm. In the ESI-MS² spectra, a series of DPIs such as *m/z* 283, *m/z* 268 and *m/z* 255 were observed in negative mode. The existence of these molecular weights verified the loss of glucose (162 Da), glucose + CH₃ (177 Da) and glucose + CO (190 Da), orderly. Its characteristic ions just like [M-H-Glu]⁻, [M-H-Glu-CH₃]⁻ and [M-H-Glu-CO]⁻ could also be

verified from the DPIs for flavonoids which have previously summarized. Therefore, DPIs mentioned above could be summarized the fragmentation regularities of group compositions and utilized for deducing the structures of related compounds from abundant complex constituents.

3.3. Comparative analysis of the main constituents existing in *Astragali radix* and SF-AP

Our previous study of liquid fermentation found that 42 constituents were attributed to saponins while the remaining 65 were identified as flavonoids [7]. However, in this report, coupled with the high-resolution mass data, obtained DPIs, retention time, standard references and related literatures, a total of 110 chemical constituents including 45 triterpene saponins and 65 flavonoids, while 109 components containing 41 triterpene saponins and 68 flavonoids were screened and identified from SF-AP and *Astragali radix*, respectively (Fig. 6). After comparing the results from SF-AP and *Astragali radix*, it could be found that the newly generated constituents after fermentation could be attributed to Azukisaponin V methyl ester, Huangqiyein F, Huangqiyein A, Huangqiyein E and Astraisoflavan-7-O-β-D-glucoside. In the meantime, Astragalus flavonoids such as Calycosin-7-O-β-D-glucoside-6''-O-butylene ester, 5,7,4'-trihydroxy-isoflavone, (3R)-7,2',3'-trihydroxy-4'-methoxy isoflavone and Calycosin were undetected after fermentation. Moreover, by comparing these two fermentation methods, it was illustrated that many more isomeric constituents could be generated from solid fermentation, while some constituents such as Pratensein and Calycosin-7-O-β-D-glucoside-6''-O-butylene ester were only observed in liquid fermentation.

It is worth noting that the most obvious change during the fermentation transversion is the relative content of some representative components. According to the experimental results (Fig. 7), it could be seen that the relative content of some constituents were increased, such as Malonylastragaloside I, Soyasaponin I, Astragaloside IV, (3R)-8,2'-dihydroxy-7,4'-dimethoxy-isoflavan, Cyclocanthoside E, Astraisoflavan-7-O-β-D-glucoside, Odoratin-7-O-β-D-glucoside, Isoquercitrin, 5'-hydroxy isomucronulatol 2',5'-di-O-glucoside, while some constituents including Astragaloside II, Astragaloside V, Formononetin, 3,9-dimethoxy-10-hydroxypterocarpan were observed with decreased relative content after the process of fermentation. Compared with the previous study of liquid fermentation, there were similar changes about the increase content of Astragaloside IV, but some other components like Cyclocanthoside E/isomers have no significant same change trend in fact.

Among them, Astragaloside IV has various pharmacological activities especially in cardiovascular diseases, digestive diseases, cancer and the other modern high incidence, high-risk diseases (Ren et al., 2013; Zhang et al., 2006). Meanwhile, Astragaloside IV is officially used as a quality-marker for *Astragali Radix* in Chinese Pharmacopoeia (2015 version). The increased content of Astragaloside IV may be due to the loss of acetyl group or glucose moiety in the fermentation transversion of Astragaloside II and Astragaloside V and the other components (Fig. 8). In this sense, it could be deduced that the transformation during the fermentation process was more conducive to playing a therapeutic effect in clinical application.

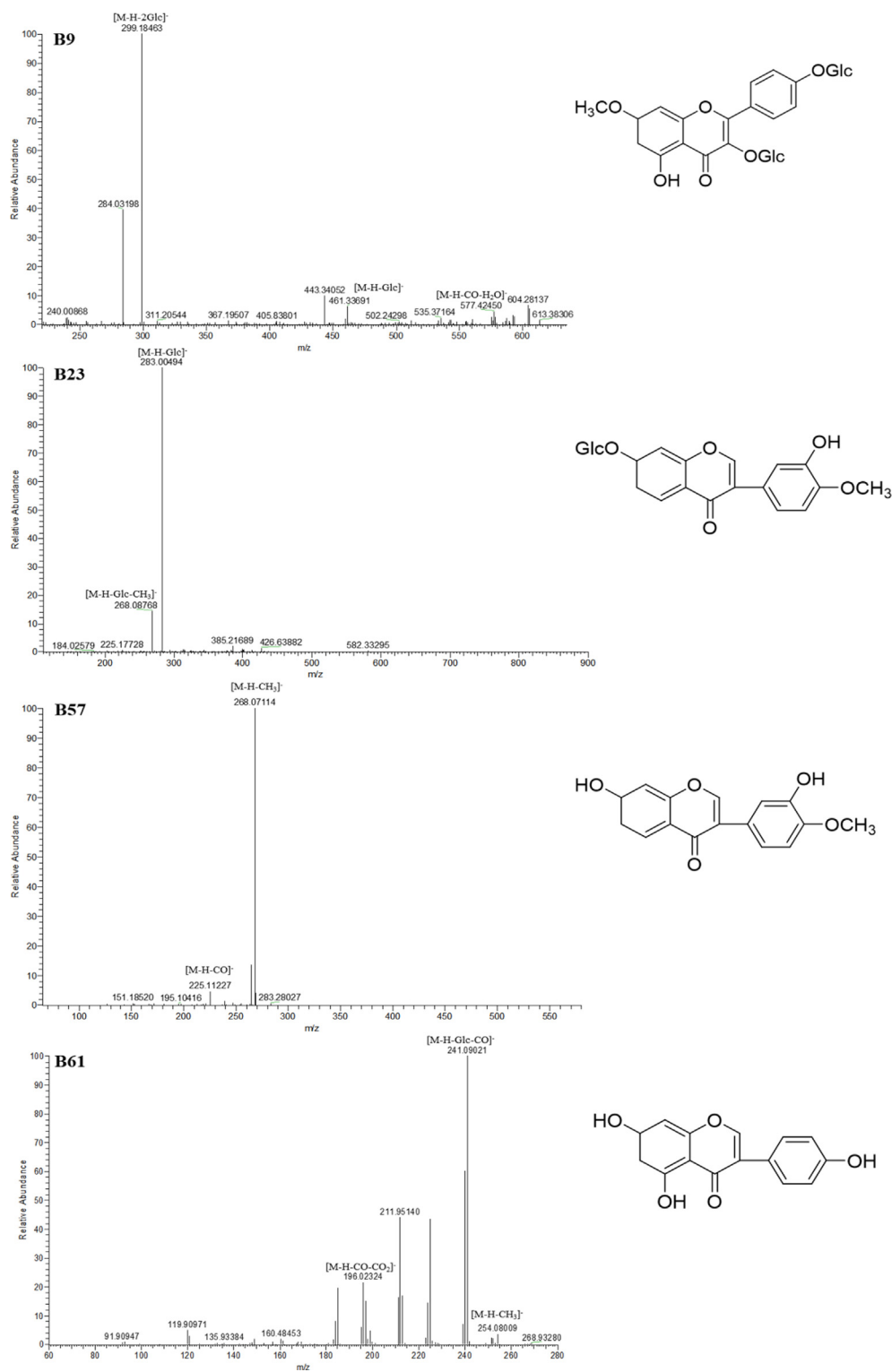


Fig. 5 The ESI-MS² spectra and chemical structures of **B9**, **B23**, **B57** and **B61**.

3.4. The antioxidative activity of *Astragali radix* and SF-AP

For further study, two kinds of antioxidative tests were chosen to evaluate the antioxidative activity of *Astragali radix* before and after solid fermentation. According to the results, the scavenging ability of the SF-AP to DPPH[•] was significantly

improved by comparing with *Astragali radix*. By selecting the mass concentration range of the samples as 0.06 ~ 0.84 mg/mL, the scavenging activity of *Astragali radix* increased from 6.21% to 36.02% while that of the SF-AP increased from 8.23% to 45.65%. In addition, with the increase of samples' mass concentration, the scavenging ability

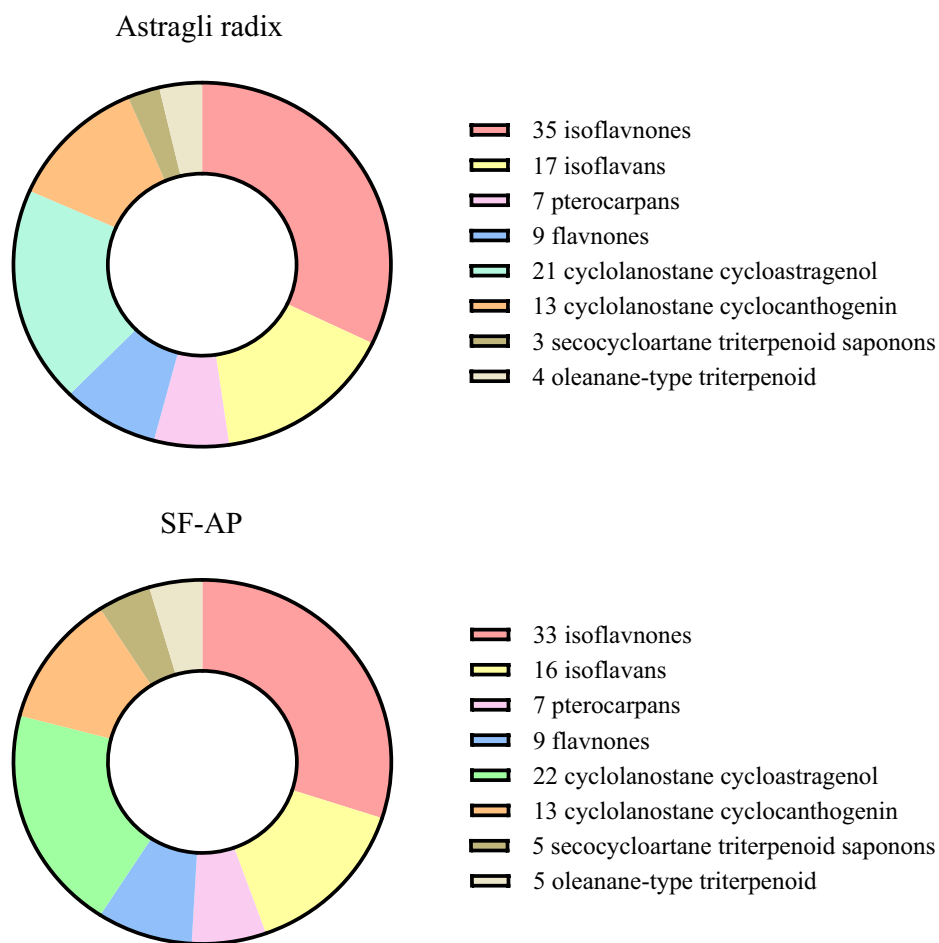


Fig. 6 The composition of constituents existing in Astragali radix and SF-AP.

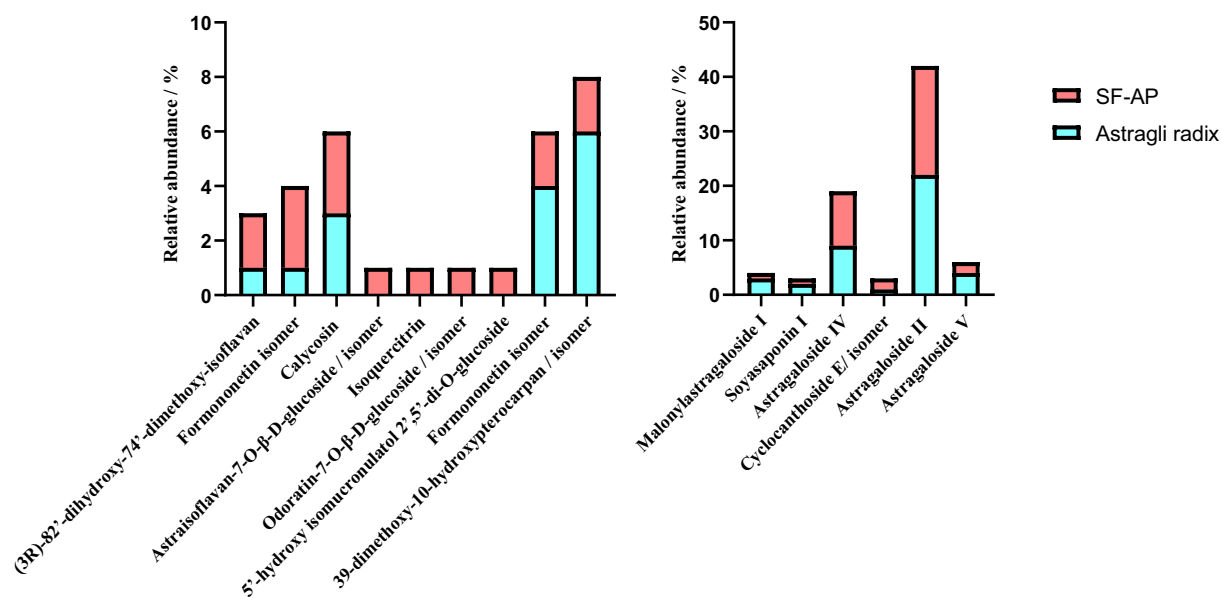


Fig. 7 The changes of representative constituents including flavonoids and triterpene saponins before and after fermentation.

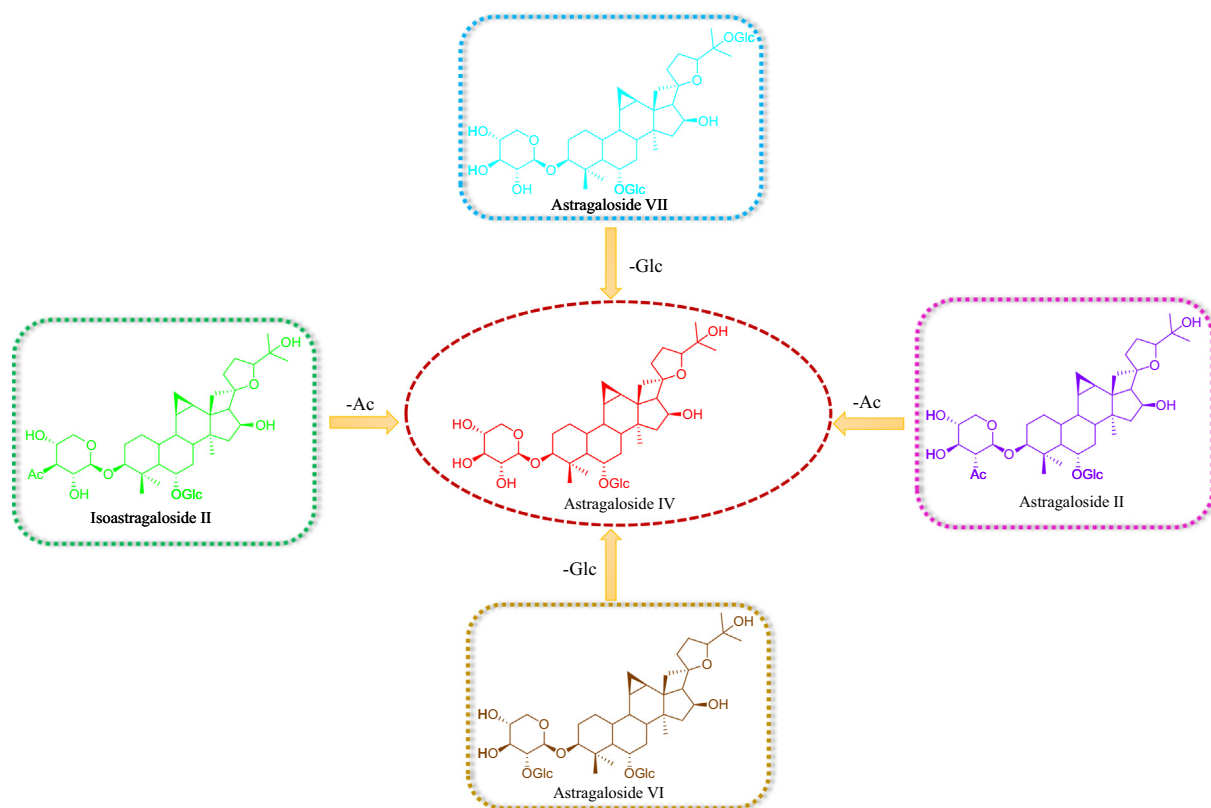


Fig. 8 The proposed transformations after fermentation.

of Astragali radix and SF-AP to $ABTS^{\cdot+}$ were enhanced. When the mass concentration was between 0.06 and 0.96 mg/mL, it could be seen that the scavenging ability of $ABTS^{\cdot+}$ of SF-AP was much higher than Astragali radix. While the mass concentration reached 0.96 mg/mL, the scavenging ability of Astragali radix to $ABTS^{\cdot+}$ was 49.5% while the scavenging ability of SF-AP was 57.4% (shown in Fig. 9).

The improvement of antioxidative activity of SF-AP is complex and a great many factors are attributed to it. What's more, some physical and chemical changes during the fermentation process played the decisive part on the antioxidative activity of Astragali radix. For instance, a varieties of sec-

ondary metabolites produced after fermentation: some methoxylated flavones lost methoxy(s) and then produced a great deal of OH-flavones; some flavonoid glycosides were hydrolyzed into aglycones, which could also increase the antioxidative activity.

4. Conclusion

In this study, UHPLC-LTQ-Orbitrap MS was used to acquire chemical profiles of Astragali radix and SF-AP. Combining with the fragmentation rules, chromatographic behavior, DPIs and related literature data, 114 compounds including 45 sapo-

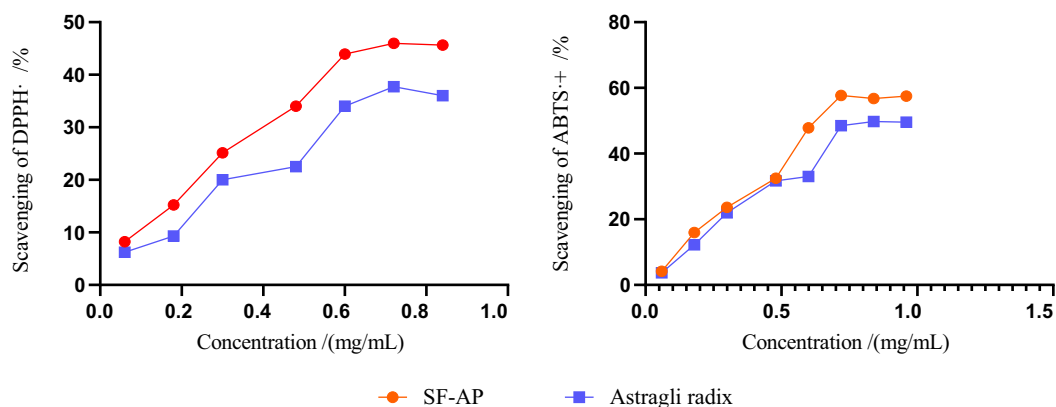


Fig. 9 The evaluation of antioxidative activity *in vitro*.

nins and 69 flavonoids were finally identified in both positive and negative ion modes. By comparison with Astragali radix, some components contained in SF-AP had significant chemical changes such as content fluctuation and isomerism owing to the occurrence of hydrolysis and other conversion reactions. Moreover, two kinds of antioxidative tests were applied to evaluate the antioxidative activity of Astragali radix before and after fermentation. The antioxidative activity of SF-AP in two kinds of antioxidative tests corresponding to the scavenging of DPPH[·] and ABTS^{·+} were both significantly higher than that of Astragali radix.

Based on the comparison of the above two aspects, fermentation can improve the internal conversion efficiency and the content of compounds, so as to improve the therapeutic effect. Although the specific chemical transformation mechanism during the fermentation process still needs further exploration, this study set a good example for the comprehensive chemical identification and much more in-depth pharmacodynamics study of the fermentation system between microbiota and Chinese herbal medicines.

Declaration of Competing Interest

The authors declare that they have no known competing financial interests or personal relationships that could have appeared to influence the work reported in this paper.

Acknowledgments

This work has been financially supported by Young and Creative Team for Talent Introduction of Shandong Province, Binzhou Medical University Scientific Research Fund for High-level Talents (2019KYQD06), Locality-University Cooperation Project of Yantai City (2019XDRHXMP18), and Independent Topic Selection of Beijing University of Chinese Medicine (2019-JYB-XSCXCY-06).

References

Chu, C., Qi, L.W., Liu, E.-Hu., et al, 2010. Radix Astragalus (Astragalus): Latest Advancements and Trends in Chemistry, Analysis. *Pharmacol. Pharmacokinet. [J] Curr. Org. Chem.* 14, 1792–1807.

Es-Safi, N.E., Kerhoas, L., Ducrot, P.H., 2007. Fragmentation study of iridoid glucosides through positive and negative electrospray ionization, collision-induced dissociation and tandem mass spectrometry[J]. *Rapid Commun. Mass SP.* 21, 1165–1175.

Fu, J., Wang, Z., Huang, L., et al, 2015. Review of the Botanical Characteristics, Phytochemistry, and Pharmacology of Astragalus membranaceus (Huangqi)[J]. *Phytother. Res. Ptr.* 28, 1275–1283.

Hsu, C.F., Peng, H., Basle, Cédric, et al, 2011. ABTS^{·+} scavenging activity of polypyrrole, polyaniline and poly(3,4-ethylenedioxythiophene)[J]. *Polym. Int.* 60, 69–77.

Hussain, A., Bose, S., Wang, J.H., et al, 2016. Fermentation, a feasible strategy for enhancing bioactivity of herbal medicines[J]. *Food Res. Int.* 81, 1–16.

Liu, D., Zhu, Y., Beeftink, R., et al, 2004. Chinese Vinegar and its Solid-State Fermentation Process[J]. *Food Rev. Int.* 20, 407–424.

Martins, S., Mussatto, S.I., Martínez-Avila, Guillermo, et al, 2011. Bioactive phenolic compounds: Production and extraction by solid-state fermentation. A review[J]. *Biotechnol. Adv.* 29, 365–373.

Ming, L., Yue-Fei, W., Guan-Wei, F., et al, 2017. Balancing Herbal Medicine and Functional Food for Prevention and Treatment of Cardiometabolic Diseases through Modulating Gut Microbiota[J]. *Front. Microbiol.* 8, 2146.

Ren, L.L., Xue, X.Y., Zhang, F.F., Wang, Y.C., Liu, Y.F., Li, C.M., et al, 2007. Studies of iridoid glycosides using liquid chromatography/electrospray ionization tandem mass spectrometry[J]. *Rapid Commun. Mass SP.* 21, 3039–3050.

Ren, S., Zhang, H., Mu, Y., et al, 2013. Pharmacological effects of Astragaloside IV: a literature review[J]. *J. Tradit. Chin. Med.* 33, 413–416.

Shang, Z., Cai, W., Cao, Y., et al, 2017. An integrated strategy for rapid discovery and identification of the sequential piperine metabolites in rats using ultra high-performance liquid chromatography/high resolution mass spectrometry[J]. *J. Pharmaceut. Biomed.* 146, 387–401.

Singhania, R.R., Patel, A.K., Soccol, C.R., et al, 2009. Recent advances in solid-state fermentation[J]. *Biochem. Eng. J.* 44, 13–18.

Stanton, C., Ross, R.P., Fitzgerald, G.F., et al, 2005. Fermented functional foods based on probiotics and their biogenic metabolites [J]. *Curr. Opin. Biotechnol.* 16, 198–203.

Wang, Y.Q., Mei, X.D., Liu, Z.H., et al, 2019a. Chemical Constituent Profiling of Paecilomyces cicadae Liquid Fermentation for Astragali Radix. [J]. *Molecules* 24, 2948–2968.

Wang, Y.Q., Liu, Z.H., Wang, S.P., et al, 2019b. Effect of Bidirectional Fermentation System of Paecilomyces cicadae /Astragalus Membranaceus of in Hyperuricemia Models and Study on Its Components[J]. *Modern Chin. Med.* 11, 012.

Wang, Z.M., Lu, Z.M., Shi, J.S., et al, 2016. Exploring flavour-producing core microbiota in multispecies solid-state fermentation of traditional Chinese vinegar[J]. *Sci. Rep.-UK* 6, 26818.

Xu, L., Du, B., Xu, B., 2015. A systematic, comparative study on the beneficial health components and antioxidative activities of commercially fermented soy products marketed in China[J]. *Food Chem.* 174, 202–213.

Zhang, J.Y., Li, N., Che, Y.Y., et al, 2011. Characterization of seventy polymethoxylated flavonoids (PMFs) in the leaves of *Murraya paniculata* by on-line high-performance liquid chromatography coupled to photodiode array detection and electrospray tandem mass spectrometry[J]. *J. Pharmaceut. Biomed.* 56, 950–961.

Zhang, Y.C., Shi, X.S., Zhang, H.M., et al, 2017. Effect of the Polysaccharides of Fermentation of Paecilomyces Cicadae for Glycyrrhiza Residue on Immune Activity[J]. *Pharm. Biotechnol.* 2, 129–132.

Zhao, C.Y., Yang, F., Qu, Q.S., et al, 2018a. Establishment of Bidirectional Fermentation System of Paecilomyces cicadae/Astragalus Membranaceus and Study on Its Components[J]. *World Chin. Med.* 13, 270–273.

Zhang, W.D., Chen, H., Zhang, C., et al, 2006. Astragaloside IV from Astragalus membranaceus Shows Cardioprotection during Myocardial Ischemia in vivo and in vitro[J]. *Planta Med.* 72, 4–8.

Zhao, W.J., Shang, Z.P., Li, Q.Q., et al, 2018b. Rapid Screening and Identification of Daidzein Metabolites in Rats Based on UHPLC-LTQ-Orbitrap Mass Spectrometry Coupled with Data-Mining Technologies. [J]. *Molecules.* 23, 151.

Zeng, W.C., Zhang, Z., Gao, H., et al, 2012. Characterization of antioxidant polysaccharides from *Auricularia auricular* using microwave-assisted extraction[J]. *Carbohydr. Polym.* 89, 694–700.